MODELING OF DIFFERENT NANO-COMPOSITE MODIFIED BITUMEN USING COMPUTATIONAL INTELLIGENCE- AN ENSEMBLE LEARNING APPROACH

A THESIS SUBMITTED TO THE GRADUATE SCHOOL OF APPLIED SCIENCES OF NEAR EAST UNIVERSITY

By
GAZI F. G. TALLAWI

In Partial Fulfilment of the Requirements for The Degree of Master of Science In Civil and Environmental Engineering

NICOSIA, 2020

GAZİ F. G. TALLAWİ MODELING OF DIFFERENT NANO-COMPOSITE MODIFIED BITUMEN USING COMPUTATIONAL INTELLIGENCE- AN ENSEMBLE LEARNING APPROACH NEU 2020

MODELING OF DIFFERENT NANO-COMPOSITE MODIFIED BITUMEN USING COMPUTATIONAL INTELLIGENCE- AN ENSEMBLE LEARNING APPROACH

A THESIS SUBMITTED TO THE GRADUATE SCHOOL OF APPLIED SCIENCES OF NEAR EAST UNIVERSITY

By
GAZI F. G. TALLAWI

In Partial Fulfilment of the Requirements for The Degree of Master of Science In Civil and Environmental Engineering

NICOSIA, 2020

Gazi F. G. TALLAWI: MODELING OF DIFFERENT NANO-COMPOSITE MODIFIED BITUMEN USING COMPUTATIONAL INTELLIGENCE- AN ENSEMBLE LEARNING APPROACH

Approval of Director of Graduate School of Applied Sciences

Prof. Dr. Nadire ÇAVUŞ

We certify this thesis is satisfactory for the award of the degree of Masters of Science in Civil and Environmental Engineering

Examining Committee in Charge:

Dr. Shaban Ismael ALBRKA — Supervisor, Department of Civil and Environmental Engineering, NEU

Assoc. Prof. Dr. Rifat REŞATOĞLU — Department of Civil and Environmental Engineering, NEU

Dr. Nasradeen Ali KHALIFA — Department of Civil and Environmental Engineering, Universiti Tun Hussein Onn Malaysia

DR. NASRADEEN ALI KHALIFA MILAD
Lecturer
Department of Civil Engineering
Faculty of Civil Engineering and Built Environmen
Universiti Tun Hussein Onn Malaysia

I hereby declare that all information in this document has been obtained and presented in accordance with academic rules and ethical conduct. I also declare that, as required by these rules and conduct, I have fully cited and referenced all material and results that are not original to this work.

Name, Last Name: GAZI F. G. TALLAWI

Signature:

Date: 5-8-2020

ACKNOWLEDGMENTS

First and foremost, I would like to express my deepest appreciation to my parents who are always there for me. Your support and trust in me inspired and encouraged me to do my best in life. Thank you for everything you have done for me.

Special thanks to my Supervisor Dr. Shaban Ismael ALBRKA, I would like to thank you for supporting me, encouraging my thesis. You were always ready to help and advise me. I'm really glad to have such a Supervisor for my thesis like you.

I got enough support and encouragement from my parents, without you, I would not be the person I am today, especially my mother and my sister Maha, who always give priority to my higher studies. My brothers, Hussam, Sultan, and my brother-in-law Osman, thank you for your love, support, and unwavering belief in me.

I am truly thankful to all my instructors at the Near East University. I appreciate them for their time, patience, and consistent help.

To my Parents…

ABSTRACT

In this study, data-driven models including MLP, ELM, LSVM, and SWLR analysis is carried out to predict the complex modulus (G*) and phase angle (δ) of polymer nano-composite modified bitumen. For this purpose, all the models MLP, ELM, LSSVM, SWLR were develop using MATLAB 9.3 (R2017a), the model input selection was presented on the correlation analysis. Subsequently, three different ensemble learning approach viz: SAE, WAE, and NNE to improve the overall efficiency with regards to prediction performance. Both the conventional, computational model, and ensemble learning techniques results were evaluated using three different performance criteria viz: determination coefficient (DC), RMSE, and R. The computation models (MLPNN, ELM, and LSSVM) shows better prediction performance than the conventional SWLR model with M2- ELM outperformed all the single computational models by producing complex modulus G* values of DC=0.9745, RMSE=0.0051 and R= 0.9872 while M2-MLPNN is better than all the models concerning the prediction of phase angle δ with values of DC= 0.9971, RMSE=0.0229 and R= 0.9985. It is indicated that all three employed ensemble methods have the ability model both G* and δ. According to prediction results NNE proved to have shown higher performance efficiency than WAE and SAE in calibration and verification phases respectively, by employing three performance indices; DC, RMSE and R.

Keywords: Extreme Learning Machine, Multi-layer Perceptron, complex modulus, phase angle, Least Support Vector Machine, Stepwise Regression analysis

ÖZET

Bu çalışmada, polimer nanokompozit modifiye bitümün karmaşık modülünü (G *) ve faz açısını (δ) tahmin etmek için MLP, ELM, LSVM ve SWLR analizlerini içeren veriye dayalı modeller gerçekleştirilmiştir. Bu amaçla tüm MLP, ELM, LSSVM, SWLR modelleri MATLAB 9.3 (R2017a) kullanılarak geliştirilmiş, model girdi seçimi korelasyon analizinde sunulmuştur. Daha sonra, tahmin performansı açısından genel verimliliği artırmak için üç farklı toplu öğrenme yaklaşımı, yani SAE, WAE ve NNE. Hem geleneksel, hesaplamalı model hem de toplu öğrenme teknikleri sonuçları üç farklı performans kriteri kullanılarak değerlendirilmiştir: belirleme katsayısı (DC), RMSE ve R. Hesaplama modelleri (MLPNN, ELM ve LSSVM) geleneksel modellerden daha iyi tahmin performansı gösterir. M2-ELM'li SWLR modeli, DC = 0.9745, RMSE = 0.0051 ve R = 0.9872 karmaşık modül G * değerlerini üreterek tüm tek hesaplama modellerinden daha iyi performans gösterirken, M2-MLPNN, değerlerle faz açısı angle tahmini ile ilgili tüm modellerden daha iyidir. DC = 0.9971, RMSE = 0.0229 ve R = 0.9985. Kullanılan üç topluluk yönteminin de hem G * hem de δ yetenek modeline sahip olduğu belirtilmiştir. Tahmin sonuçlarına göre NNE, üç performans indeksi kullanarak, sırasıyla kalibrasyon ve doğrulama aşamalarında WAE ve SAE'den daha yüksek performans etkinliği gösterdiğini kanıtladı; DC, RMSE ve R.

Anahtar Kelimeler: Aşırı Öğrenme Makinesi; Çok katmanlı Algılayıcı; karmaşık modül; faz açısı; En Az Destek Vektör Makinesi; Kademeli Regresyon analizi

TABLE OF CONTENTS

ACKNOWLEDGMENTS .... **i**
ABSTRACT .... **iii**
ÖZET .... **iv**
TABLE OF CONTENTS .... **v**
LIST OF FIGURES .... **viii**
LIST OF TABLES .... **ix**
LIST OF ABBERVIATIONS .... **x**

CHAPTER 1:INTRODUCTION **1**
1.1 Introduction 1
1.2 Problem Statement 3
1.3 The Objective of Study 3
1.4 Significant of Study 4
1.5 Thesis Organization 4

CHAPTER 2:LITERATURE REVIEW **6**
2.1 Introduction 6
2.2 The Properties of The Binder 6
2.3 Bituminous Mixture and Materials. 7
2.4 Pavement Distresses 7
2.4.1 Fatigue Distresses 8
2.4.2 Bleeding Distresses 8
2.4.3 Raveling Distresses 8
2.4.4 Rutting Distresses 8
2.5 Application of Bitumen 9
2.6 Types of Bitumen 9
2.6.1 Penetration Grade Bitumen 9
2.6.2 Oxidized Bitumen 9
2.6.3 Cutback Bitumen 10
2.6.4 Bitumen Emulsion 10
2.7 Modification of Bitumen 10

2.8 Polymer Materials and Modified-Bitumen 11
2.9 Nanomaterials Modified Bitumen 12
2.10 Artificial Intelligence in The Field of Bitumen Binder 14

CHAPTER 3:MATERIALS AND METHODOLOGY 19
3.1 Multilayer Perceptron Neural Network (MLPNN) 19
3.2 Extreme Learning Machine (ELM) 21
3.3 Least Square Support Vector Machine (LSSVM) 23
3.4 Step-Wise-Linear Regression (SWLR) 26
3.5 Ensemble Learning Technique (ELT) 26
3.5.1 Linear Ensemble Approach 27
3.5.2 Nonlinear Linear Ensemble (NLE) Approach 28
3.6 Proposed Modeling Procedures 30
3.7 Data Normalization and Performance Evaluation 32
3.8 Experimental Procedures 33
3.8.1 Materials and Properties 33
3.8.2 Dynamic Shear Rheometer 34

CHAPTER 4:RESULTS AND DISCUSSION 36
4.1 Results of Data-Driven Models 36
4.2 Results of Multi-layer Perceptron Neural Network (MLPNN) 39
4.3 Extreme Learning Machine (ELM) 43
4.4 Results of Least Support Vector Machine (LSVM) 45
4.5 Results of Stepwise Regression analysis (SWLR) 47
4.6 Ensemble Learning Results 49

CHAPTER 5:CONCLUSIONS AND RECOMMENDATION 52
5.1 Conclusion 52
5.2 Recommendation 54

REFERENCES 55

APPENDICES **64**
Appendix 1: The Data Used in The Modeling. 64
Appendix 2: Ethical Approval Latter 81
Appendix 3: Similarity Report. 82

LIST OF FIGURES

Figure 1.1: The overall structure of the thesis 5

Figure 3.1: Three-layer multilayer perceptron structure 21

Figure 3.2:ELM structure 23

Figure 3.3: Least Square Support Vector Machine (LSSVM) 26

Figure 3.4:Schematic of Simple Averaging Ensemble 28

Figure 3.5: Schematic Structure of Weighted Average Ensemble 28

Figure 3.6: Schematic Structure of Neural Ensemble Method 29

Figure 3.7: Ensemble Techniques 30

Figure 3.8: Proposed Methodology of data driven models 31

Figure 3.9: Schematic presentation of DSR 35

Figure 4.1: Correlation Analysis between the experimental variables for δ 38

Figure 4.2: Correlation Analysis between the experimental variables for G* 38

Figure 4.3: Network topology for M1 and M2 model combination 40

Figure 4.4: Error function of MLPNN for (a) M1 and (b)M2 for (G*) 41

Figure 4.5: Scatter plots showing the experimental versus predicted for (a) G* (b) (δ) ... 43

Figure 4.6: Point to point plots of the experimental vs predicted value for (a) G* (b) (δ) . 45

Figure 4.7: Radar charts of the experimental vs predicted value for (a) DC (b) R………. 46

Figure 4.8: Error function of MLPNN for (a) M1 and (b)M2 for (G*) 48

Figure 4.9: Point to point plots of the experimental vs predicted value for (a) G* (b) (δ) . 49

Figure 4.10: Radar charts of the experimental vs predicted value for (a) DC (b) R 51

Figure 4.11: Error function of ensemble for RMSE 51

LIST OF TABLES

Table 3.1: Physical properties of samples 33

Table 4.1:Statistical Analysis of the variables 37

Table 4.2: Correlation Analysis between the experimental variables 37

Table 4.3: Input variable combination 39

Table 4.4: Performance results of MLPNN model for (G*) and (δ)................................ 40

Table 4.5: Performance results of ELM model for (G*) and (δ)..................................... 44

Table 4.6: Performance results of SVM model for (G*) and (δ)..................................... 46

Table 4.7: Performance results of SWLR model for (G*) and (δ) 47

Table 4.8: Performance results of three types of ensemble model for (G*) and (δ)......... 50

LIST OF ABBERVIATIONS

NSC:	Normal Strength
HSC:	High-strength concrete
EVA:	Ethylene-vinyl acetate
ASTM D36:	Standard Test Method for Softening Point of Bitumen
ASTM D5:	Standard Test Method for Penetration of Bituminous Materials

CHAPTER 1

INTRODUCTION

1.1 Introduction

Bitumen is highly temperature susceptible which means its physical and chemical properties change when subjected to various temperature conditions (Kim, 2008). Also, viscoelastic substances like Bitumen are not behaving directly, regarding some of their properties such as stiffness which act as a function of strain or stress. Bitumen is made of complex mixtures of aromatic, aliphatic and naphthenic hydrocarbons with a small amount of metallorganic and other organic. To provide better performance characteristics and properties of bitumen to implementing in a good manner in the practical site and to facing the problems happens regarding maintenance if disjointedness in layers, and incompatibility with the modifier (Paliukait et al. 2014; Read, et al., 2003). Polymers can be sub-grouped as elastomers and plastomers. Elastomers are favourable modifiers of asphalt cement (AC) at low temperatures, while plastomers are more suitable modifiers at high temperature. Typical polymers used in the bitumen modification include Styrene-Butadiene-Styrene (SBS), Ethylene-vinyl acetate (EVA), Natural rubber (NR) and Polypropylene (PP) (Firouzinia & Shafabakhsh, 2018; Ziari et al., 2018).

Bitumen is the material complex properties made from unpolished lubricant and/or with natural bitumen in the manner of at all or closest to solubility, solid in weather-based temperature as effectively waterproofed, glue and violate. Bitumen is, a dark brown colored hydrocarbon obtained as a byproduct of the distillation of crude oil, is mostly used in pavement construction due to its viscoelastic and adhesive properties, (Kok et al., 2010). On this basis to providing an understanding of getting bitumen properties taking consideration from its self-procedure of the production process and from unpolished lubricant characters in which more content of lubricant will determine higher bitumen characters. Dynamic Shear Rheometer (DSR) is used in the assessment of rheological properties of bitumen binders at intermediate and high temperatures. Dynamic shear modulus (G*) which is considered as the resistance of the material to deformation under repeated shear loading and the phase angle (δ) which is defined as the lag between the applied shear stress and the resulting shear strain are the two parameters revealed upon oscillatory shear testing performed by DSR (Abedali et al., 2015). These parameters are further used in the assessment of rutting and fatigue resistance which are the most common mechanisms of failure in bitumen pavement. It is favorable that, bitumen binders demonstrate stiff behavior at high temperatures and low frequencies and elastic behavior at low temperatures and high frequencies to prevent rutting and fatigue failures (Bala et al., 2018).

As a result of the limitations of Bitumen regarding the temperatures, various types of modifiers such as plastic, polymers, and Nano-materials were added to the base bitumen to improve the performance of the bitumen mixture (Cuadri et al., 2011), therefore in order to improve rheological properties, bitumen modification with polymeric materials is a common practice and referred to as polymer modified asphalt cement (PMAC). Unique properties of nanomaterials such as high surface work, a significant fraction of surface atoms, structural features, quantum effects, and spatial confinement are some of the features that promoted the improvement of binder properties in terms of stiffness and also leads to higher temperature susceptibility and improved strength of bitumen against moisture damage (Saltan et al., 2018). Nanomaterials have also shown to enhance the incompatibility problem of polymer and base asphalt, associated with the occurrence of phase separation. Common nanomaterials used in this purpose included nanosilica, nanoclay and carbon nanotubes (Ezzat, H., et al; Ziari et al., 2018)

According to previous studies in the literature, enhancement in the performance of bitumen modified with nanomaterials in terms of improved complex modulus and reduced phase angle have indicated that better rutting resistance performance is achieved (Yang et al., 2013). However, the field of nanomaterial in the bitumen modification still requires a significant amount of research before field application. In this way, understanding the behavior and chemical processes that takes place during the modification process is of paramount importance in the field of nanomaterial modified bitumen binders (Xiao et al., 20110; Filonzi et al.2018). At default laboratory experimentation of AC is a time and resource-intensive process. Therefore, many researchers have attempted to develop mathematical and computational models to predict performance characteristics of AC to assist with the experimental procedures. As acknowledged in the literature, the physical and chemical properties of bitumen binders have a strong influence on the performance characteristics of AC (Venudharan et a., 2017). However, the relationship was not in high correlation. Instead, test conditions such as temperature and frequency were highly correlated with the performance characteristics (Behnood et al., 2019)

1.2 Problem Statement

It is a well known fact that enhancing the quality of bitumen mixture varies modifiers like polymers and nano-materials were used. As a result of the high cost of some materials and failure in laboratory equipment with associated which has a high cost as well. That creates a limited number of works and studies that have been recognizing the performance of modified bitumen with nanomaterial. It can be noticed that the field of nanomaterial in the bitumen modification still requires a significant amount of research before field application, while most of the studies which have been done to bitumen binders modified with polymer nano-composite materials are limited to be addressed by experimental investigations especially in artificial intelligence (AI) computational modeling in this matter requires further study. Consequently, these AI were implemented in this study using physical properties of, bitumen modified with polymer and polymer nano-composites at various concentrations and test conditions as a predictor and the performance characteristics indicator, complex modulus (G*) as the predicted variable to find out the behavior of Bitumen modified with polymer and polymer nano-composite materials at the first stage of the work. The literature showed that despite the growing application of AI-based modeling but still it was associated with some weaknesses that would results in low accuracy due the overfitting or underfittings, for example, artificial neural network (ANN) is prone to overfit.in this regards this study introduced a novel approach called ensemble learning techniques in order to boast the prediction accuracy of the AI model.

1.3 The Objective of The Study

The objectives of the study are to:

- ✓ To an insight about the different recently evolutionary AI-based model, for example, Multi-layer Perceptron (MLP), Extreme Learning Machine (ELM), Least Support Vector Machine (LSVM), and Stepwise Regression analysis (SWLR)
- ✓ To employ the MLP, ELM, LSSVM, and SWLR models to predict the complex modulus (G*) and phase angle (δ) of polymer nano-composite modified bitumen

- ✓ To develop a comparison study between the MLP, ELM, LSSVM, and SWLR models and the experimental results.
- ✓ To apply three ensemble techniques viz: simple average ensemble (SAE), weighted average ensemble (WAE), and neural network ensemble (NNE) to improve the overall efficiency of the prediction performance.

1.4 Significant of Study

As a result of the outflow of the studies that have been discussed the performance of modified bitumen with nanomaterial and the studies which have been conducted to bitumen binders modified with polymer nano-composite materials are limited to be addressed only by experimental test therefor the results of the study will be of great benefit to the pavement field by finding the viscoelastic properties of modified bitumen cement at elevated temperatures and frequencies using Multi-layer Perceptron (MLP), Extreme Learning Machine (ELM), Least Support Vector Machine (LSVM), and Stepwise Regression analysis (SWLR) models in the modeling process and showing the capability and efficiency of this applications to deal with Complex behavior of pavement materials. The literature showed that despite the growing application of AI-based modeling but still it was associated with some weaknesses that would results in low accuracy due to the overfitting or underfittings, for example, artificial neural network (ANN) is prone to overfit.in this regards this study introduced a novel approach called ensemble learning techniques in order to boast the prediction accuracy of the AI model. To best our knowledge, this thesis is the first work to introduce a novel ensemble technique in the field of bitumen and the prediction of G*.

1.5 Thesis Organization

- Chapter one is explaining the introduction about the topic, problems statement as well as the objectives of the research
- Chapter two is addressing the previous researches that were conducted on or related to the study area
- Chapter three is providing in detail the methods and procedures that carried on to achieve the objectives of the study
- Chapter discusses the results of the research
- Chapter five is about the conclusion, recommendation and future studies

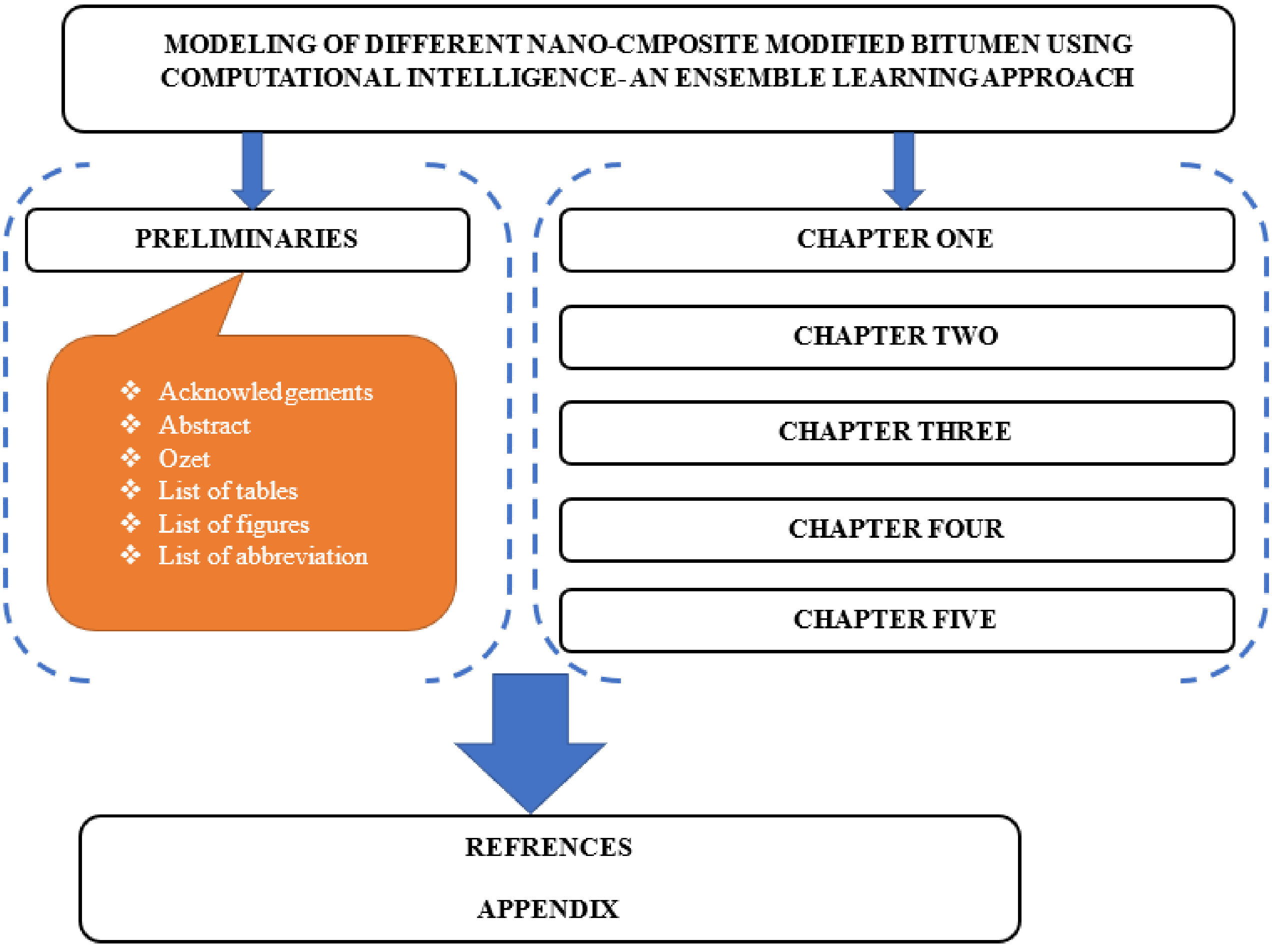

Figure 1.1: The overall structure of the thesis

CHAPTER 2

LITERATURE REVIEW

2.1 Introduction

The concept behind this chapter is to review the previous works and literature related to bitumen, bitumen binder, artificial intelligence models, polymer materials, different categories of bitumen, and nano-composite modified asphalt. However, a review of several tasks related to modifiers in bitumen mixtures. Bituminous materials are a hydrocarbon which obtained as a product of the distillation of crude petroleum or found in natural deposits (Read & Whiteoak, 2003).All bituminous materials consist primarily of bitumen and have strong adhesive properties, it has the capacity adhere to a solid surface in a fluid stat depending on the surface's nature, while the adhesion could be prevented by adding water to the surface, therefore the Bitumen is water-resistant, the flow or viscous properties of bitumen change according to stress and temperature conditions. The failure, or loss of the desirable properties of bitumen, can be noticed it takes the form of hardening. Resultantly, a decrease in flow and adhesive properties and an increase in the coefficient of thermal expansion and the softening point temperature (Mochinaga et al., 2006). All bituminous materials have colors ranging from dark brown to black. Also, asphalts are thermoplastic materials, meaning that they liquefy when heated and solidify when cooled (Ali et al., 2017). To check the efficiency of the Bitumen in the site, designing the physical properties of the binders is very fundamental. There to find out the properties of Bitumen the following testing methods are carried out: Direct Tension (DTT), Pressure aging vessel (PAV), Rolling Thin film Oven (RTFO), and Bending Beam Rheometer (BBR) etc.

2.2 The Properties of The Binder

In general, the binder properties of pavement structure will govern the rheological performance of modified bitumen binders by making influences on the viscous-elasticity characteristics of bitumen materials (Lee, 2006).Thus, the flow of viscous properties of bitumen change according to stress and temperature conditions. Resultantly, a decrease in flow and adhesive properties and an increase in the coefficient of thermal expansion and the softening point temperature (Mochinaga et al., 2006). All bituminous materials have colors ranging from dark brown to black. Also, asphalts are thermoplastic materials, meaning that they liquefy when heated and solidify when cooled (Ali et al., 2017). Van der Poel (1954) investigated the behavior of bitumen for suitable binder characters in the form of graphic characters, which functional behaviors depend on temperature and frequency. Regarding this finding even if, the not applicable for complex stress-strain behavior of bitumen researcher were tried to simulated the graphic properties to provide linear behavior of bitumen in viscous-elasticity relation by applying rheological parameters (Jong pier et al., 1969; Hall, 1972; Ossa, 200). In the complex behaviors of viscous-elasticity, the temperature has a critical impact considering the time of traffic loading to determine the value of stiffness and elastic, which is at low temperature solid stiff and high-temperature liquid elastic. This makes viscous-elasticity as changeover unit is named viscosity.

2.3 Bituminous Mixture and Materials.

In bituminous materials contain mainly of bitumen and have strong adhesive properties. Those Bituminous materials are a hydrocarbon obtained as a product of the distillation of crude petroleum or found in natural deposits (Read & Whiteoak, 2003). It can adhere to a solid surface in a fluid stat depending on the surface's nature, while the adhesion could be prevented by adding water to the surface; therefore, the Bitumen is water-resistant. In addition, bitumen applied in bitumen mixed pavement due to its performance, economical, increase Adhesive Nature, melts at a low point, its Rheological and Physical Properties produce Flexibility, recycled, and diversity colors. In this manner to use the specific bitumen the criteria to differentiate is on the safety, inconsistency with the durability, physical properties, and solubility. The performance of bitumen may not be satisfactory in all situations of weathering effect as checked-in accelerated weathering system feature. To check the effective performance of bitumen in the practical area understanding the fundamental binders designing physical properties under weathering affects.

2.4 Pavement Distresses

The pavement may face Too many distress some of them may occur according to the chemical and physical properties of the bitumen binder, while the other may occur by the weather conditions and the loads which applied by the tracks. In general, different types of distresses of bitumen in flexible pavements happen according to the natural and physical properties of the bitumen binder, while the other possible occurrences are the weather conditions and the loads which applied by the tracks. Stable deformation is considered as one of the main distresses of bitumen that occurs in flexible pavements when subjected to natural and physical properties of the bitumen binder, traffic load, and weathering effects. In most of the time, the bitumen distress occurs due to rutting in to two main factors of pavement as weakness of sub-layer put under the pavement structure, which is structural rutting and as the fails of bitumen mixture properties of design due to the lack of controlling the vertical load exerted makes fails shear strength, which is non-structural rutting. The distresses are as the following:

2.4.1 Fatigue Distresses

Cracking: is the principal structural distress, the layer materials and thicknesses of pavement, applied loads the consistency of the bitumen cement, the Bitumen content and the air voids and aggregate characteristics of the bitumen concrete mix are the factors which affect the development of fatigue(El-Basyouny & Witczak, 2005).

2.4.2 Bleeding Distresses

This refers to the accumulation of bitumen cement material around the surface of the pavement. It starts accumulating by an individual drop and subsequently aggregates into a sticky and shiny film. Bleeding shows surface friction which can be considered as a potential safety hazard. Bleeding occurs as a result of insufficient mixing between the cement and air which creates a void as the bitumen cement is expanding (Xu & Huang, 2012).

2.4.3 Raveling Distresses

Raveling is occurred by the continued infiltration of water and the break downing of a bitumen top layer. When the water is presented on the top layer of bitumen and sunlight will start to damage the bitumen surface by breaking the bond between the aggregate and bitumen. it will affect the bitumen surface losing its impermeable properties and will let water enter the surface. When water begins to enter into a bitumen surface it will lead to further cracks then the pavement failure occurs (Adlinge & Gupta, 2013).

2.4.4 Rutting Distresses

Rutting is channelled depressions in bitumen surface. When the deformation takes a place only in the bitumen concrete it may occur by plastic flow or consolidation. Bitumen cement stiffness is a big influence for rutting resistance of bitumen mixes while the Stiffer bitumen cement can increase rutting resistance (Xiao, Amirkhanian, & Juang, 2007).

2.5 Application of Bitumen

Bitumen has been used since the old civilization until now due to its natural resources, it can be used in the different field for humans needs such as waterproofing in sealing flat roofs and roofing felt, while most of the Bitumen produced used in pavement field due to the following reasons (Yildirim, 2007):

- Production of Bitumen is economical
- Rheological and Physical Properties of it bring Versatility
- Bitumen melts at a low point
- Bitumen can be Recycled
- Bitumen increase Adhesive Nature
- Bitumen has a diversity Colors

2.6 Types of Bitumen

The specification of Bitumen to displays the safety, the disparity with the durability, physical properties, and the solubility. The Bitumen can be categorized into the following grade types:

2.6.1 Penetration Grade Bitumen

Penetration Grade Bitumen, there is a kind of refinery bitumen which is manufactured at various viscosity. Usually, the penetration analysis is done to characterize the bitumen according to its hardness. And hence called penetration bitumen. Penetration grades range from 15-450 for road asphalt. Though, the commonly used range is between 25-200. This can be achieved through the distillation procedure control test. The needed hardness may be acquired through the application of partial control fluxing the residual Bitumen with the oils (Read & Whiteoak, 2003).

2.6.2 Oxidized Bitumen

The filter Bitumen is further managed by inserting the produced air. The way the oxidized Bitumen is produced. By preserving an adjusted temperature, the air is inserted under pressure into smooth Bitumen. by the reaction of the components of Bitumen and this introduced oxygen, a Compounds of higher molecular weight are formed. The Maltenes and the Asphaltenes content helps in increasing the harder mix. The mix which has a temperature sensitivity and a less ductility. This type of Bitumen is commonly used in manufacturing fields such as covering for pipes and ceiling. By this way of producing, the Bitumen which has a less penetration can be produced, it can be used in the pavement (Loeber, Muller, Morel, & Sutton, 1998).

2.6.3 Cutback Bitumen

This type is called to the Bitumen when it has a grade less than penetration grade, it has a decreased viscosity for a specific time by inserting of volatile oil. the Bitumen gain back its normal viscosity when the volatile materials are evaporated after the application. The penetration grade Bitumen can be classified as a thermoplastic material. It demonstrates the various value of viscosity for various temperature. In the site of the road industry, it is requisite for the materials to be a liquid shape in surface dressing phase. By cutback asphalt, the material can earn back its normal rigidity after casting. By increasing the temperature, the liquidity can be for any Bitumen. cutback Bitumen is used when there is a need to have fluidity for any Bitumen at lower temperatures in the surface dressing phase (Lamperti, 2011).

2.6.4 Bitumen Emulsion

This kind of Bitumen has 2 phase system with 2 immiscible fluids. The first one is scattered like specific globules included in the other fluid. This kind of Bitumen is obtained once the separate globules of bitumen are separated from a continuous form of water. An emulsifier having a long hydrocarbon series with an anionic or cationic ending is applied for receding the Bitumen globules. This type supplies an electrochemical climate. The ionic section of the series has an attraction to the water and the Bitumen is attracted by hydrocarbon section. This Bitumen is conducted by using sprays also the viscosity has the main attention. when the content of the Bitumen is increased, the viscosity of the mixture increased. The stability of emulsions relies on the Water evaporation rate, the types of Bitumen emulsifier and its quantity, the Mechanical forces, and the Bitumen globules size (Brown & Needham, 2000).

2.7 Modification of Bitumen

The pavements issues have an undesirable effect on the safe side for beings and to the economic side for the society particularly the countries where financial resource for pavement maintenance is often insufficient and due to the restrictions of bitumen about the temperatures, modification of bitumen is one of the best techniques to develop the properties of bitumen different types of modifiers such as polymers, plastic, still slag and glass, additional to the base bitumen to advance the performance of the bitumen mixture (Cuadri, Partal, Navarro, García-Morales, & Gallegos, 2011). Thus, The convention of modified bitumen gives the capacity to regulator the limits of mechanical stability of road surfacing by enhancing the properties of some types of surfacing during hard extremely conditions of services (Sarsam & Lafta, 2014). By using modifiers with bitumen showed increasing in performance by raising the cohesion of the bitumen, and increase the viscosity and decrease the thermal capability of the binder (Al-Khateeb & Al-Akhras, 2011). Some studies conducted that by using a minimum of 10% of modified bitumen leads to longer enduring streets with better execution (Sabadra, 2017).

Several studies conducted to modified bitumen and it concluded that by adding modifiers to bitumen its heat and strength resistance to reach the double and that leads to improving the shearing resistance it also showed that the density of modified bitumen is more than the density of the base bitumen and it gains by increasing the content of modifiers so the water saturation, respectively, reduces (Kishchynskyi, Nagaychuk, & Bezuglyi, 2016). In addition, Sarsam and Lafta studied a different type of modified asphalts to find out the physical properties of it and, obtained result showed that by adding the modifiers to the base asphalt, the penetration value of bitumen cement decreased, while the Softening point of bitumen cement gained and Ductility of bitumen cement decreased (Sarsam & Lafta, 2014).

2.8 Polymer Materials and Modified-Bitumen

The polymer is a chemical compound with molecules and bond together to create a long repeating chain. It can be used in a different field due to its unique properties (Sabadra, 2017). Polymers widely used as modifiers for binder it can be classified as the following: plastomers, thermoplastic elastomers, and reactive polymer, it can enhance the thermal capability of bitumen binders, each one of them has its particular impact according to their properties: Thermoplastic elastomers increase the resistance of the binder to fatigue by improving the elastic properties, reactive polymers and plastomers increase the resistance to deformation and also increase the stiffness, (Brasileiro et al., 2019).

Application of polymer modified bitumen showed the ability to intensification the resistance of the mixture against rutting and thermal cracking. Furthermore, the incompatibility between the bitumen and polymers leads to phase segregation among the blends which deuced the strength of pavement (Ali et al., 2017). By modifying the bitumen with polymer, the polymers differ the viscoelastic properties and the strength of the Asphalt, by providing the ductility, improve the Fracture strength, increase the elastic response and improve the cohesive property (Yildirim, 2007). And a study conducted by (Becker et al., 2001) the results indicated that the polymer used as modifiers in paving field due to its capability to enhance the physical properties of the binders, the introduction of polymer improves the rutting resistance, high temperature sensitivity, fatigue, stripping and thermal cracking. Mostly it's used when durability and high performance are necessary (Becker & Méndez, 2001).

In the rheological properties of polymers elastomeric, the main role in the modified bitumen is to govern elasticity of pavement to control and repel the constant deformation as rutting effect, develop bitumen strength in collaborating the structure and to minimizing the extreme cold weathering cracking due to low temperature (Robinson, 2005). In this manner, the polymers will reunite the structure of unmodified bitumen binders together to decrease the phase angle to provide more flexible elastic modified bitumen binders for long service life within good performance quality under the weathering effects (Airey, 2003).

Several studies conducted to polymer modified bitumen showed that when the polymer is added to bitumen it increases the softening point and imparts a high elasticity to bitumen. On the other hand, it showed that the mixture has a lower temperature sensitivity (Kochanski et al., 2016). In general, the high cost of the polymer modifiers is the reason that affects a wide use of it and to improve the bonding of polymer elements, between themselves and with bitumen, plasticizer was added in a polymer composition in some situations (Kishchynskyi et al., 2016).

2.9 Nanomaterials Modified Bitumen

Many studies have been done to explore the utilize of nanomaterials as a modifier for asphalt, and they found that when nanoparticles are added to the binder, the viscosity and the cohesion of bitumen can be increased, which mean the mixture may have a good performance under high-temperature conditions (Ezzat et al., 2016; Fang et al., 2013).

For example; Abdelrahman et al., (2014) made an experimental on the NC-bitumen nano-composite. The indicated results showed that Nano clay modification of bitumen enhances the physical properties of asphalt. Raising Nano Clay concentration in the binders increase the temperature susceptibility of asphalt, as well as rising the complex modulus while decreasing phase angle.

Jahromi & Khodaii. (2009) demonstrated a comparative rheological test on the base bitumen and nanoclay modified bitumen. The outcomes showed that the presence of nanoclay can change the rheological properties of bitumen by decreasing the phase angle and increasing the stiffness, it showed the capability to improve ageing resistances(Jahromi & Khodaii, 2009).

Amirkhanian et al., (2010) studied and predicted the rheological properties of the binders containing various percentages of carbon nanoparticles under high temperatures. Their test resulted that the viscosity of binders increased as the rate of nanoparticles increased, also an increase in failure temperature was noted, but the percent increase depends on the binder-grade, phase angles were consistently reduced, the addition of the particles resulted in more resistance to deformation and higher elasticity, while elastic and viscous modulus values showed an increase with the addition of nanoparticles.

You et al. (2011) on the effects of nano -clays on the rheological properties of bitumen by blending surfactant- modified Nano-clay at Two percent and four percent by weight of asphalt. It was found that the addition of nano-clay increases the viscosity of the base binder across varying temperatures. Also, the nanoclay-modified bitumen showed that the phase angle was decreased while the complex modulus was increased which mean the binder has a good performance under high temperature.

The previous studies have reported that the performance of bitumen modified with nanomaterials shows that the complex shear modulus of modified bitumen improved while the phase angle decreased, indicating that the permanent deformation (rutting) of modified bitumen could be minimized (Ali et al., 2017). Ezzat et al. (2016) to evaluate the Bitumen Binders Modified with Nanoclay and Nanosilica, it concludes that the mixture resistance to permanent deformation could be improved using the proper amount of nanomodified and, the nanomodified bitumen can be stored to be used after few days it can be up to 10 days without a big effect on its properties obtained by modification process in the bingeing.

The nanomaterials have been introduced as another way to improve the properties of bitumen and enhance the compatibility among the bitumen and polymers. Nanomaterials have been developing and incorporated rapidly in the field of bitumen mixture as it has unique properties. These properties include high surface work, a large fraction of surface atoms, structural features, quantum effects, and spatial confinement (Saltan et al., 2018). In the predicting study of Ali et al., (2017) that modification of bitumen with nanomaterials would improve the properties of bitumen including an increase of stiffness of bitumen which leads to be less susceptible to the temperature and improve the strength of bitumen against moisture damage. Some nanomaterials have been used to modify polymer modified bitumen such as; nanoclay, nanofibers, carbon nanotubes and nanosilica (Ali et al., 2017).

It can be noticed, although Nano-materials are promising, some type of Nano-materials are expensive and demands further research to exploring and optimizing the enhancement in the binder properties before field testing and applications (Ezzat et al., 2016). In addition to this, due to the limitation of time and the high cost of the materials and experiments, also the leakage in equipment therefor some studies were conducted to predict the behavior of modified Bitumen using computational intelligence /Artificial intelligence models to solve the different type of real-life procedures in engineering and environmental field shows its products and capabilities by dealing with a non-linear characteristic. AI applications can be used in the modeling of different real-life procedures in the field of engineering due to their predictive capacities and nonlinear characteristics (Asadi et al., 2014).

2.10 Artificial Intelligence in The Field of Bitumen Binder

Nanomaterials have also shown to enhance the incompatibility problem of polymer and Bitumen, associated with the occurrence of phase separation. Common nanomaterials used in this purpose include nano silica, nanoclay and carbon nanotubes (Ezzat et al., 2016; Yang & Tighe, 2013; Ziari, Amini, Goli, & Mirzaeiyan, 2018). According to previous studies in the literature, enhancement in the performance of bitumen modified with nanomaterials in terms of improved complex modulus and reduced phase angle have indicated that better rutting resistance performance is achieved (Xiao, Amirkhanian, & Amirkhanian, 2010)

However, the field of nanomaterial in the bitumen modification still requires a significant amount of research before field application. Performance of nanomaterial modified bitumen have also been acknowledged in the literature by a limited number of studies (Firouzinia & Shafabakhsh, 2018; Ziari et al., 2018). However, bitumen binders modified with polymer nano-composite materials have been only limited to be addressed by experimental investigations and the reality of AI modeling in this matter requires further study. Despite it some works have been done in AI-based modeling for instance;

Cüneyt Aydin, A., et al (2006), 2 ANFIS models were used: HSC data and NSC data to predict the elastic modulus of concrete. The ANFIS results were compared with codes and some data obtained from the literature and the study was concluded that ANFIS is a good tool for modeling and predicting the complex modulus of bitumen and it showed the ability to evaluate the elements affecting complex modulus of bitumen before it moves to the site which will help to save time consumed.

Tapkın et al. (2009) presented a study to predict the strain accumulation in polypropylene (PP) modified marshal specimens. The data observed from repeated creep tests were modeled in ANN and demonstrated positive similarities with the experimental observation results. The significance of their study was that for a specific type of bitumenmixture and predefined testing conditions the cumulative strains at the end of repeated Load creep tests could be conducted without applying destructive tests (Tapkın et al., 2009).

Xiao et al. (2011) developed a series of ANN models to predict the viscosity values of crumb rubber modified (CRM) binders. Their results indicated that the ANN-based models were able to predict the viscosity of CRM binders, and also, the models are applicable to other types of rubber.

Xiao et al (2011) in one of their studies which involves the usage of serial ANN models to predict the viscosity rate of a crumb rubber modified (CRM) binders. The result of the study showed that ANN models can be used in predicting the viscosity of CRM binders. Furthermore, these models can be used in prediction using another kind of rubber types.

Yilmaz, M et al (2011), ANFIS was used to model the complex of base and ethylene-vinyl-acetate (EVA) polymer modified bitumen. The data was obtained from a dynamic shear rheometer (DSR) test. In the modeling process the EVA content, bitumen temperature, and frequency were the inputs data and the complex modulus was the output data. The ANFIS result was closely related to the actual the results they conclude their study that ANFIS can be used for modeling the complex modulus of bitumen under varying temperature and frequency and it is an important method to evaluate the factors affecting it and Adaptive Neuro-Fuzzy Inference System can be considered as good tools which help reduce the time consumed.

Pourtahmsb et al. (2015) investigated to replicate the performance of hot bitumen mix with in different polymer by analysis the resilient modulus using ANFIS modeling. The system input was concrete aggregate recycling, stone mastic bitumen within different concentrations and temperature as a defining factor. Their evaluation was based on the statics indicator of R^2, RMSE, and R and found HMA within SMA predict were accurate regarding the experimental result and failed of HMA within RCA achieved.

Moghaddam et al. (2015) to investigate the prediction of the deformation: rutting characteristic performance of modified bitumen mixture by analysis polyethylene terephthalate PET using ANFIS modeling. The analysis to formulate input defined factor is tested temperature, stress level, PET concentration. From their assessment based on RMSE and they conclude as predict were increasingly good for the input analysis of bitumen mixture.

Shafabakhsh and Tanakizadeh (2015) to search the resilient modulus under the effect of loading features in the time interval by formulating the indirect tensile test result using ANFIS. The system analyses were temperature and loading period as defined factors. Their evaluation based on the fraction of the rest period to the loading period and found that MR was improved within decreasing of temperature, which shows the prediction is capable to reduce the cost expensive and time loss for the experimental test.

Taher et al., (2015) employed ANFIS for prediction of the rutting performance of Polyethylene Terephthalate (PET) modified bitumen mixture. The process, which simulates the mixture's deformation, was constructed with (ANFIS). The inputs were PET percentages, stress levels and temperatures.

Khademi et al (2016) used three artificial intelligence techniques: Artificial Neural Network (ANN), Adaptive Neuro-Fuzzy Inference System (ANFIS) and Multiple Linear Regression (MLR) to predict the 28 days compressive strength of concrete using 14 different input variables. The obtained result that ANN and ANFIS models efficient in predicting the 28 days compressive strength of concrete and are recommended due to its high efficiency especially when high accuracy is needed. (Khademi, Jamal, Deshpande, & Londhe, 2016).

Khashman and Akpinar, (2017) used ANN model to predict and classify compressive strength the results proved the possibilities of using the ANN model.

Venudharan and Biligri (2017), employed an Artificial Neural Network to predict rutting performance of bitumen with different Crumb Rubber (CR) ranges. The input parameters were considered as five different CR gradations, base binder viscosity, frequency, and test temperature. (Venudharan & Biligiri, 2017).

Abedali (2018), conducted a comparison study between the performance MLR and ANN with base bitumen considering temperature, frequency, dynamic viscosity, shear stress and strain as inputs and G* as output.

Lui et al. (2018) have attempted to predict the dynamic modulus of virgin bitumen mixtures and bitumen mixtures containing recycled bitumen shingles with data from four different projects. The input parameters included were sieve test results on aggregates, air voids, effective binder content, the viscosity of the bitumen binder, loading frequency, and recycled bitumen board contents. The suggested ANN model was compared with the low model and gave significantly higher prediction veracity than the low model (Liu, Yan, Liu, & Zhao, 2018).

Firouzinia and Shafabakhsh. (2018), it was stated that the bitumen mixtures are highly temperature susceptible and sole enhancement of binder rheological properties are not sufficiently able to overcome this problem. Thus additives should be applied in bitumen mixtures. In their study, the impact of Nano-silica addition at five different contents was investigated on the thermal sensibility of hot mix bitumen using experimental procedures and the ANN models. It was found that modifying bitumen mixtures with Nano-silica improved the temperature sensitivity and the ANN models were generated with 5 input parameters of the percentage of the void, aged sample situation, bitumen type, bitumen situation and temperature with training algorithm as Radial Basis Function (RBF) Which show the capability to give an accuracy result (Firouzinia & Shafabakhsh, 2018).

Alas and Shaban, (2019) employs ANN to predict the G* and δ the results showed the reliability of ANN in predicting the above parameters.

Michele et al., (2019) In this study, declared that the chemical composition of base bitumen for its modification like polymers/additives improve aspects of neat bitumen properties and lead to compatibility problems in storage and production.

CHAPTER 3

MATERIALS AND METHODOLOGY

3.1 Multilayer Perceptron Neural Network (MLPNN)

MLPNN as one of the types of artificial neural networks (ANN) belongs to the learning machine family, which uses a computational approach to develop predictive models for desired parameters by simulating the way biological neurons work in the human brain (Liu, J., et al., 2018). MLPNN can be illustrated in Fig 3.1. The function of a hidden node has overcome the intricacy involved in the process numerous types of ANN have been adopted in the literature. A multilayer perceptron (MLPNN) was adopted in this study. With this type of ANN, the learning is supervised, which indicates that for a given set of input vectors, the output vectors are provided to the network and the system is expected to adjust its weights using forward and backward calculations to minimize the prediction errors, which is also known as the learning phase.

The structure of MLP is divided into three layers, which are strongly interconnected with artificial neurons. The initial layer is the input layer x_i where the input signals are stored for a given set of input parameters x_{ai}. Input parameters in this study were the physical properties of the blends (penetration value and softening point) and mechanical test parameters (temperature and frequency).

$$x_i = (x_{1i}, x_{2i}, \dots \dots \dots x_{ai}) \qquad i = 1, \dots \dots, n \qquad (3.1)$$

The final layer is the output layer y_i, where the targeted parameter, G*, was expected to be predicted in this study.

$$y_i = (y_{1i}, y_{2i}, \dots \dots \dots y_{bi}) \qquad i = 1, \dots \dots, n \qquad (3.2)$$

The intermediate layer is called the hidden layer and it is devoted to the calculations that formally connect the input layer x_i with the output layer y_i.

A weighted sum of the values of the input variables is computed through the weights that are associated with each connection by eqn. 3.3;

$$y = \sum_{i=1}^{a} w_i x_i + w_0 \qquad (3.3)$$

Where w_i is the weight associated with the i^{th} input parameter, x_i is the data corresponding to the input parameter and w_o is the bias.

The output value is calculated in a forward pass using a transfer function. Numerous transfer functions such as the Heaviside step function, sigmoidal, or hyperbolic tangent have previously been used in the literature. Utilization of the activation function is highly dependent on the nature of the dataset and the type of model desired to be developed. In this study, a hyperbolic tangent as expressed in Eqn. 3.4 was adopted.

$$f(a) = \frac{e^{a}-e^{-a}}{e^{a}+e^{-a}} = \frac{2}{1+e^{-2a}} - 1 \qquad (3.4)$$

The abovementioned procedure is an iterative process. The network performs a series of forwarding and backward calculations to adjust its weights to achieve the most accurate predictions to the target values, which is also called the training of the neural network (Baldo, Manthos, & Pasetto, 2018). In this study, MATLAB (MathWorks Inc R2020a) was used to develop ANN models. Although various training algorithms are available in MATLAB, the selection of the training algorithm depends on the type of neural network to be modelled and the structure and complexity of the data to be fed to the network. The Levenberg-Marquardt (LVM) training algorithm was observed to be the most suited algorithm considering the structure of the dataset observed from the DSR oscillation tests. Figure 3.1 below the structure of the MLPNN neural network applied.

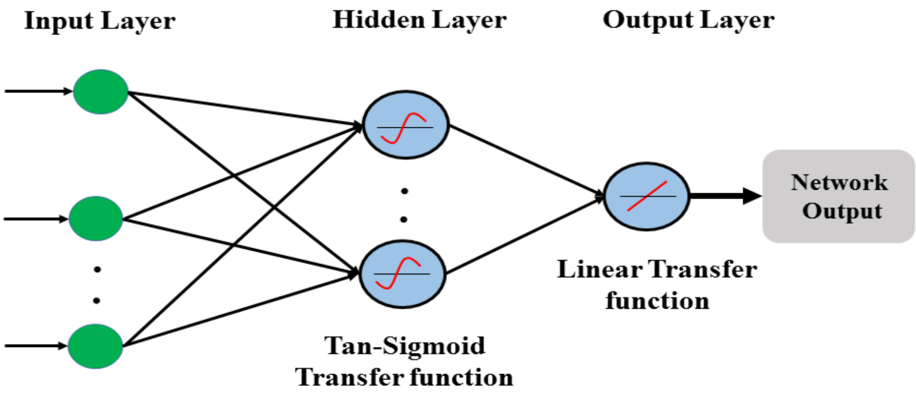

Figure 3.1: Three-layer multilayer perceptron structure

3.2 Extreme Learning Machine (ELM)

Normally, traditional ANN model requires that the parameters of the hidden neuron are tuned. Recently, ELM was established as a novel method that can be used in mapping it features despite the requirement of a traditional ANN(Yaseen et al., 2016). From several pre-assigned neurons in the ELM, the predictors, as well as the hidden neurons, are randomly computerized. These values do not have to pass through all the neurons. More also, the generalization ability of these method needs minimum computational time.

As a recently evolving computational algorithm, the ELM was first proposed by Huang et al. (2006) and is comprised of a single hidden layer feedforward network (SLFN). The ELM is relatively unlike from the conventional feed-forward neural network (FFNN) (Huang et al., 2006; Huang et al., 2015). Notably, the potential of the ELM could be attributed to the fast learning speed and its generalization ability(Huang et al., 2006; Huang et al., 2015).

For the development of the ELM model in this study, it was done using the training data

$\{(x_1, y_1), \ldots, (x_t, y_t)\}$ Whereby x_t defined as the explanatory and y_t is defined as the response variable.

As such, the descriptive variables (input vector) signified as $x_1, x_2, \ldots, x_t$ well-defined as the vector $y_1, y_2, \ldots, y_t$ represent the observed. For a set of N training samples (i.e. $t =$

$1, 2, \ldots, N$) in which $x_t \in \mathbb{R}^d$ and $y_t \in \mathbb{R}$, an SLFN with H hidden nodes is mathematically stated as [19]:

$$\sum_{i=1}^{H} B_i \, g_i(\alpha_i . x_t + \beta_i) = z_t, \tag{3.5}$$

whereby $B \in \mathbb{R}^H$, $Z(z_t \in \mathbb{R})$ and $G(\alpha, \beta, x)$ are described as forecasted weights which are found in the output layer, output model as well as the activation function.

as [42]:

$$G(x) = \frac{1}{1+exp\,(-x)}, \tag{3.6}$$

For ELM the output is presented in a linear form, whereby suitable number of the hidden neuron, this can result in minimizing the error to the lowest possible value as shown in equation 15 (Huang et al., 2006):

$$\sum_{t=1}^{N} \|z_t - y_t\| = 0, \tag{3.7}$$

$$Y = GB \tag{3.8}$$

in which

$$G(\alpha, \beta, x) = \begin{bmatrix} g(x_1) \\ \vdots \\ g(x_N) \end{bmatrix} = \begin{bmatrix} g_1(\alpha_1 . x_1 + \beta_1) & \cdots & g_L(w_H . x_1 + \beta_H) \\ \vdots & \cdots & \vdots \\ g_1(\alpha_N . x_N + \beta_1) & \cdots & g_L(w_H . x_N + \beta_F) \end{bmatrix}_{N \times H} \tag{3.9}$$

and

$$B = \begin{bmatrix} B_1^T \\ \vdots \\ B_H^T \end{bmatrix}_{H \times 1} \tag{3.10}$$

and

$$Y = \begin{bmatrix} y_1^T \\ \vdots \\ y_N^T \end{bmatrix}_{N \times 1} \tag{3.11}$$

Whereby G is indicated as the concealed layer yield, T is the transpose of the framework. The yield loads Bˆ can be evaluated by reversing the network of the concealed layer utilizing Moore-penrose summed up converse capacity (+):

B ̂=G^+ Y   (3.12)

In the long run, the assessed qualities yˆcan be controlled by:

$$\hat{y} = \sum_{i=1}^{H} \hat{B}_i \, g_i(\alpha_i . x_t + \beta_i) \qquad (3.13)$$

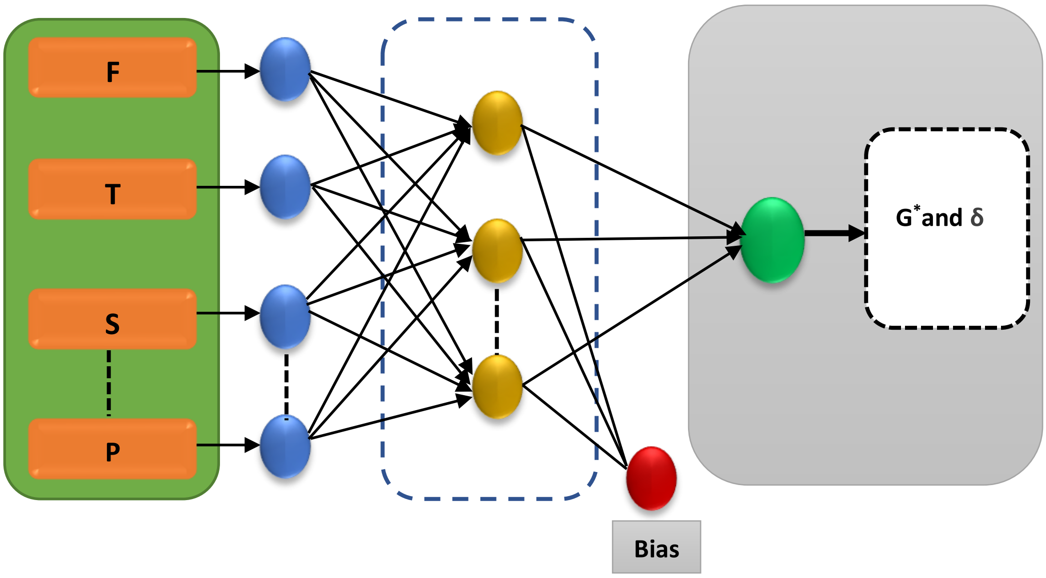

Figure 3.2: ELM structure

Where F is the frequency, T is the temperature, S is the softening point and Penetrations.

3.3 Least Square Support Vector Machine (LSSVM)

LSSVM model is an advanced algorithm form that offers various computational improvement, which minimizes numerous burdens. The LSSVM is a special SVM model that gives alternative through the conversion of the quadratic optimization problems to a linear system of equations (Nourani et al., 2018). The LSSVM can equally be applied in solving both regression and classification issues. A short explanation of the model is shown below. Whereby its architecture is indicated in Figure 3.3. Considering the predictors x_i and output y_i, while the non-linear function is demonstrated as follows:

$$f(x) = w^T \varphi(x) + b \tag{3.14}$$

Whereby *f* demonstrates the connection between the indicators and predictand and w, and b are the m-dimensional weight vector, planning capacity and predisposition term, individually. By utilizing the estimation blunder work, the issue of the relapse issues is demonstrated as far as the basic minimization rule as:

$$\min J(w,e) = \frac{1}{2} w^T w + \frac{\gamma}{2} \sum_{i=1}^{m} e_i^2 \tag{3.15}$$

which is subjected to the following constraints:

$$y_i = w^T \varphi(x_i) + b + e_i \text{ (i=1, 2,…, m)} \tag{3.16}$$

whereby γ is defined as penalty term and e_i as training error for x_i.

To discover answers for w and e, the Lagrange multiplier ideal programming strategy is utilized to tackle Equation (3). The target capacity can be controlled by adjusting the obliged issue into an unconstrained issue. The Lagrange work L can be communicated as

$$L(w,b,e,\alpha) = J(w,e) - \sum_{i=1}^{m} \alpha_i \left\{ w^T \varphi(x_i) + b + e_i - y_i \right\} \tag{3.17}$$

where α_i are the Lagrange multipliers.

Karush-Kuhn-Tucker (KKT) situations can be taking into consideration, the optimum condition can be achieved through taking the derivatives of Eq. (5) partially in regards with *w*, *b*, *e* and α, respectively as.

$$
\begin{cases}
w = \sum_{i=1}^{m} \alpha_i \varphi(x_i) \\
\sum_{i=1}^{m} \alpha_i = 0 \\
\alpha_i = \gamma e_i \\
w^T \varphi(x_i) + b + e_i - y_i = 0
\end{cases}
\tag{3.18}
$$

$$
\begin{bmatrix} 0 & -Y^T \\ Y & ZZ^T + I/\gamma \end{bmatrix} \begin{bmatrix} b \\ \alpha \end{bmatrix} = \begin{bmatrix} 0 \\ 1 \end{bmatrix}
$$

(3.1)

By defining the kernel function $K(x, x_i) = \varphi(x)^T \varphi(x_i), i = 1,...,m$, which is satisfied with Mercer's condition, the LSSVM can be represented as

$$
f(x) = \sum_{i=1}^{m} \alpha_i K(x, x_i) + b
$$

(3.20)

$$
K(x, x_i) = \exp(-\| x - x_i \|^2 / 2\sigma^2
$$

(3.21)

Before the calibration, the local rainfall values as well as the input parameters are normalized using their corresponding standard deviation and mean. The values obtained from the normalization were further used for the calibration of the model. In the LSSVM training period, generally, the grid-search process is utilized in estimating the optimum of the variables. This grid-search process has the ability to yield optimum parameters. The application of cross-validation process has the capability of preventing downscale modelling from the problem of over fittings.

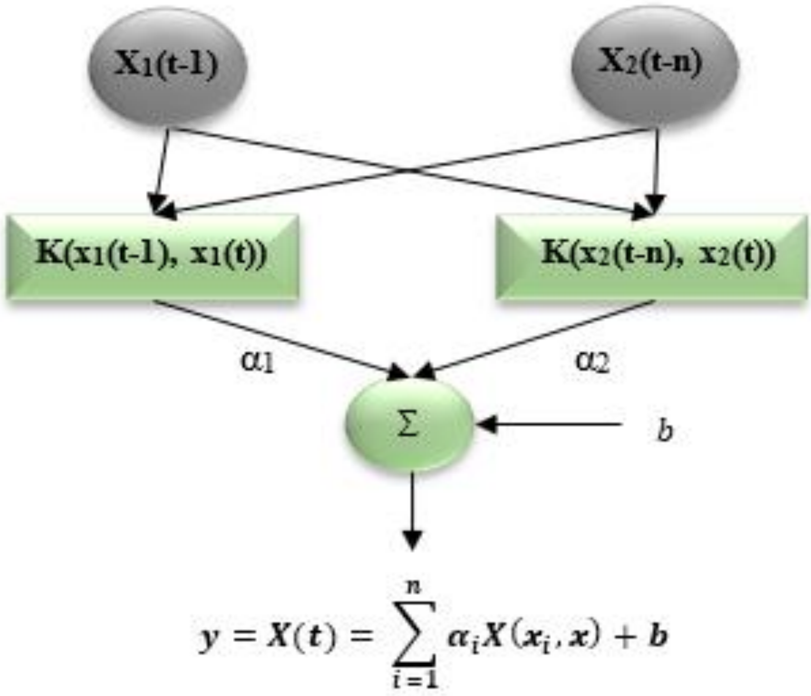

Figure 3.3:LSSVM structure

Where X_1 and X_2 are the respective input of the models (Here are F, T, P, and T)

3.4 Step-Wise-Linear Regression (SWLR)

Generally, LR is one of the major approaches in modelling various variables (input and output variables). It is of paramount importance to note that while showing the correlation that exists between single and multiple variables in finding the optimal set of the parameters, which gives the highest prediction efficiency, which is related to the output variable (Yasar et al., 2012). Based on Çevik, (2007) in describing the systematic regression as a forward selection method that chose the optimal set of the input variables by deleting or adding the variables through the influence of the residual sum of the squares. Step-Wise-Linear Regression (SWLR) follow systematic modification of the variables through checking the impact of every variable. Each variable that does not contribute and satisfy the base mechanism of model, then that variable will be deleted step wise until it impacts it's no longer present (Yasar et al., 2012). The theory of SWLR can be demonstrated through MLR (Wu et al., 2020; Zhang et al., 2016). The method of deleting or adding an input inconstant from the LR is considered as systematic regression (Lachniet and Patterson, 2006).

3.5 Ensemble Learning Technique (ELT)

The ability to combine models (ensemble technique) to improve the final prediction has been successful in various fields including classification, hydro-environmental, water resources and traffic engineering (Abba et al. 2019). ELT is a discipline in the field of machine learning used to combine the process of obtaining multiple predictors by single models to enhance the final prediction performance. The main target of the ensemble is to produce higher accuracy and reliable estimates than could be achieved through a single model. Other researchers have categorized the ELT into two, namely homogeneous and heterogeneous ensembles; when ELT comprised of the same learning algorithm (e.g. neural network), it is called homogeneous, but if it consists of different learning algorithms, it defined as heterogeneous. As suggested by (Elkiran et al., 2019) the heterogeneous ensemble is recommended for overcoming the model diversity and for attaining prediction accuracy. Therefore, two linear (i.e. simple averaging ensemble (SAE) (see, Fig. 3.3) and weighted averaging ensemble (WAE)) (see, Fig. 3.4) and one nonlinear technique, namely NN-E were employed in this thesis to simulate the G*and δ.

3.5.1 Linear Ensemble Approach

The proposed SAE approach is carried out by considering the arithmetic average of the predicted model's outputs (of MLPNN, ELM, LSSVM, and SWLR) as:

$$G * and\ \delta_{(t)} = \frac{1}{N} \sum_{i=1}^{n} G * and\ \delta_{(t)i} \tag{3.22}$$

Similarly, the WAE approach can be obtained by assigning a unique weight to each of the individual outputs, and the final predicted outcomes are obtained by averaging the models. The WAE

provides more reliable predictive skills than the SAE owing to the nature of assigning weights, and it can be expressed as:

$$G * and\ \delta_{(t)} = \sum_{i=1}^{N} w_i G * and\ \delta_{(t)i} \tag{3.23}$$

where w_i is the assigned weight on the output of the i^{th} model,**G^* and δ** *(t)* is the ensemble output (SAE or WAE), $G * and\ \delta_{i(t)}$ is the output of i th single model (here outputs of MLPNN, ELM, LSSVM, and SWLR) and N is the number of single models (here, N=4).

where w_i can be computed as:

$$w_i = \left[\frac{DC_i}{\sum_i^N DC_i}\right] \tag{3.24}$$

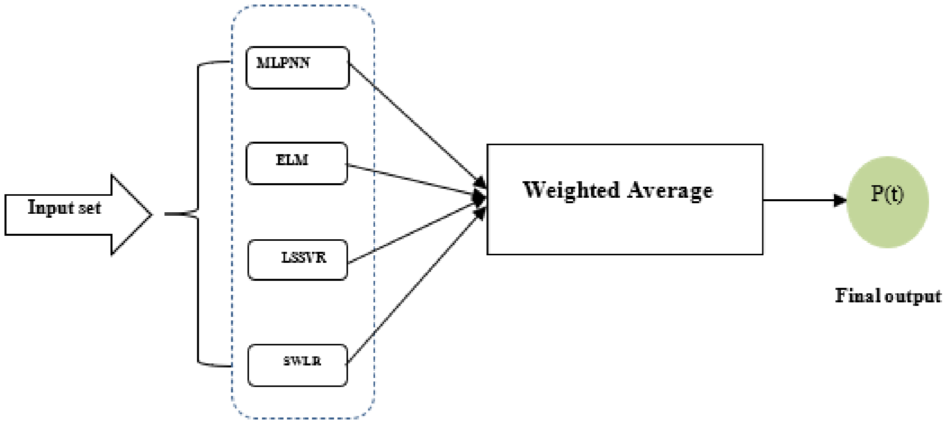

Figure 3.4: Schematic of Simple Averaging Ensemble

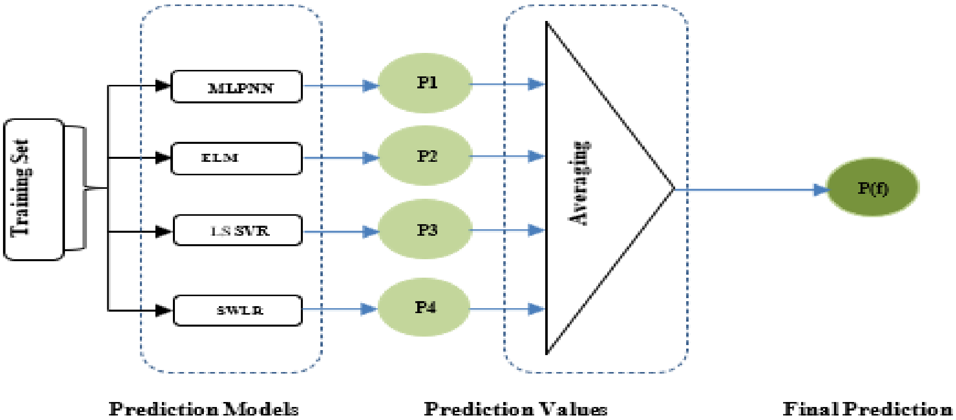

Figure 3.5: Schematic Structure of Weighted Average Ensemble

3.5.2 Nonlinear Linear Ensemble (NLE) Approach

The approach of NLE is similar to the traditional NNE model where the outputs of the single models, i.e. LSTM, ELM, GRNN, and HW models are imposed and trained using a new neural network (NN). The procedure follows the same trend of the traditional NN in terms of best architecture selection. Recently, the application of the NN ensemble has received attention in different fields of hydro-environmental engineering, including earth-fill dam seepage analysis (Sharghi et a., 2018), vehicular traffic noise (Nourani et al., 2020) etc, and all have reported the superiority of the NLE over the single model. Moreover, the above studies suggest the use of other nonlinear kernel functions as an alternative for such nonlinear ensembling. Hence, this study proposes an ensemble using the HW model as the additional nonlinear kernel function due to its advantages for single modeling prediction. Although the ensemble learning model has not previously been used in complex modulus (G^*) and phase angle (δ) prediction, this model has shown significant potential in water resources research [61]. Fig. 3.5 shows the schematic of the proposed NLE techniques using the NNE model.

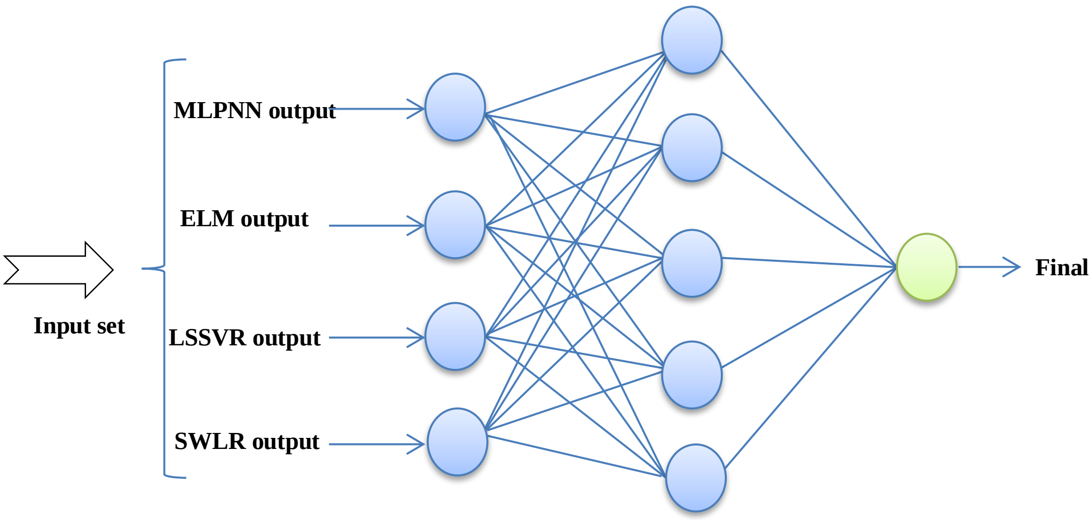

Figure 3.6: Schematic Structure of Neural Ensemble Method

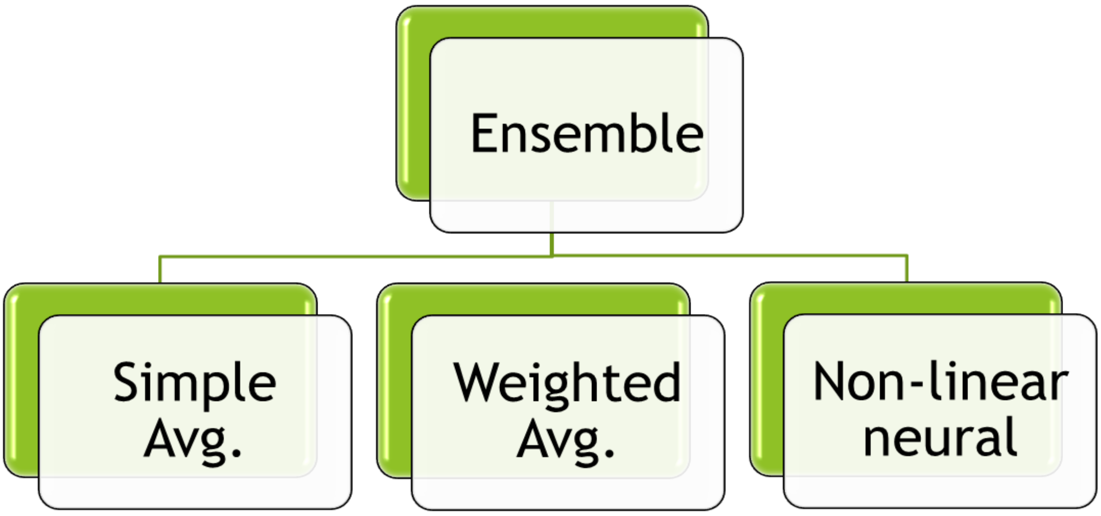

Figure 3.7: Ensemble Techniques

3.6 Proposed Modeling Procedures

In this study, data driven models including MLPNN, ELM, LSSVM, and SWLR is carried out to predict the complex modulus (G*) and phase angle (δ) of polymer nano-composite modified bitumen for the first scenario. The second scenario comprises of three different types of ensemble learning these were employed to boost the accuracy of the prediction. The inputs of those models are softening point, penetration, Temperature, and frequency. The data were observed from a dynamic shear rheometer (DSR) test. The resulted G* and (δ) from the three data driven approach will be compared with the experimental result. The conclusion can be drawn based on comparing their performance. The main proposed method by which the test was performed is shown in Figure 3.7 below. A set of 381 data points from six different blends of AC at different concentrations were used in the modelling of three data driven models (MLPNN, ELM, LSSVM, and SWLR), the data is provided in Appendix 1. Furthermore, 285 (75%) of the data points were used for training the network, 96 (25%) of the data points were used for testing the models. The reason why checking data set for the model validation was used is to stop and minimized the overfitting of the training data set, therefore a validation data set is used to check and control the potential for the model overfitting the data. The testing data set has significance since it shows the prediction capacity of the network for the untrained data set.

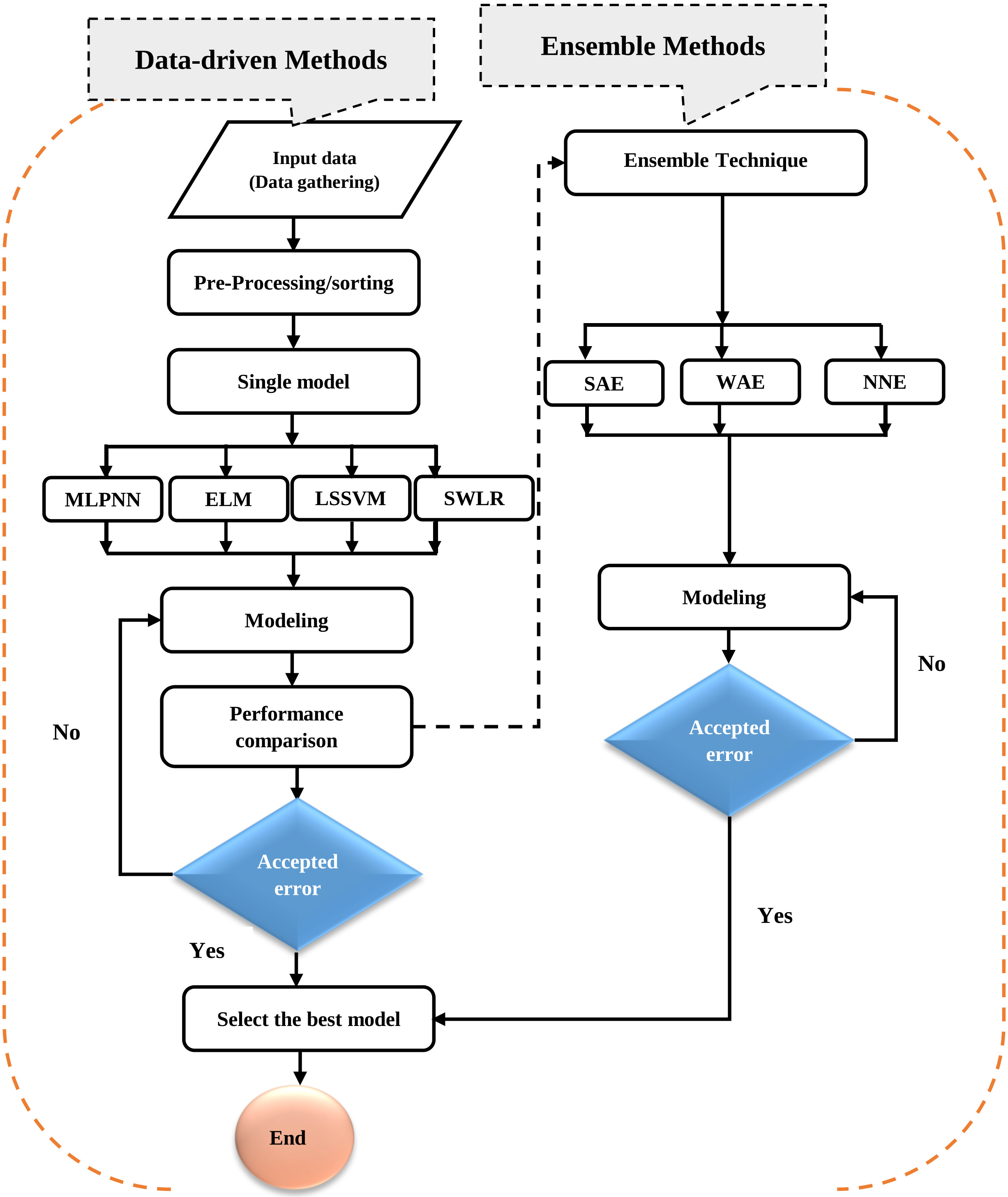

Figure 3.8: Proposed Methodology of data driven models

3.7 Data Normalization and Performance Evaluation

To maintain and make sure that equal priority and attention was given to both the input as well as the output, and also to reduce their dimensions, the data applied in this research was scaled in the range between 0 to 1. The major advantage of normalizing the data prior to the introduction of Al models is to reduce data redundancy and to reduce or minimize the larger numerical errors (Sola & Sevilla, 1997). The data employed in this research was normalized using Eqn. 3.12 prior to NNE, SVM and MLR modelling.

$$X_n=\frac{x-x_{min}}{x_{max}-x_{min}} \tag{3.25}$$

The data driven models (NNE, SVM and MLR) models developed with training and testing data sets were evaluated for their prediction capacity using the performance indicator metrics. Coefficient of determination (DC), RMSE and R were the common statistical performance indicators adopted in various studies (El-Badawy et al., 2018; Kok et al., 2010; Liu et al., 2018).). R^2 and RMSE as expressed in Eqn. 3.13 and 3.14 were adopted in this study.

$$DC = 1 - \frac{\sum_{j=1}^{N}\left[(Y)_{obs,j}-(Y)_{com,j}\right]^2}{\sum_{j=1}^{N}\left[(Y)_{obs,j}-\overline{(Y)}_{obs,j}\right]^2} \tag{3.26}$$

$$RMSE = \sqrt{\frac{\sum_{i=1}^{N}(Y_{obsi}-Y_{comi})^2}{N}} \tag{3.27}$$

$$R = \frac{\sum_{i=1}^{N}(Y_{obs}-\bar{Y}_{obs})(Y_{com}-\bar{Y}_{com})}{\sqrt{\sum_{i=1}^{N}(Y_{obs}-\bar{Y}_{obs})^2}\sum_{i=1}^{N}(Y_{com}-\bar{Y}_{com})^2} \tag{3.28}$$

Where N, Y_{obsi}, $\bar{Y}$ and Y_{comi} *a*re data number, observed data, the average value of the observed data and computed values, respectively.

3.8 Experimental Procedures

3.8.1 Materials and Properties

The base bitumen utilized was of 80/100 penetration grade. ASA in the form of white powder was used as the polymer modifier at 5% concentration to the weight of base bitumen. Two different nanomaterials, namely Nano copper and Nano calcium, were obtained from a company in China and mixed with ASA at 3% and 5% compositions to form two different binders modified with polymer composites. Samples were prepared using a high shear mixer at a constant temperature of 170 ^{o}C and at a speed of 5000 rpm for 90 minutes to make homogeneous mixtures. Evaluation of the physical properties of the unmodified, polymer modified and polymer nano-composite modified binders were conducted by penetration (ASTM D5) and softening point (ASTM D36) tests. Physical properties of the binders were also used as input parameters in computational modelling. Findings are presented in Table3.1

Table 3.1: Physical properties of samples

Material	**Penetration (dmm)**	**Softening point (^{o}C)**
Bitumen 80/100	82	46
5% ASA	74	50
3% ASA-Nano copper	66.4	56
5% ASA-Nano copper	69.1	55
3% ASA-Nano calcium	75.3	55
5% ASA-Nano calcium	76.9	53

3.8.2 Dynamic Shear Rheometer (DSR)

A DSR was used to observe the rheological properties of modified binder samples mentioned in the Materials and Properties section above. The test is conducted at temperatures from 46 ^{o}C to 82 ^{o}C with increments of 6 ^{o}C as specified in Superpave PG guidelines. Temperature control of the samples was achieved by a fluid bath system and temperature control unit to keep temperatures constant and uniform over the range of temperatures in which the experiments were conducted. The DSR equipment shown in Figure 3.8 consists of top and bottom plates. Samples of 1-mm thickness were sandwiched between 25-mm diameter plates, where the bottom plate was fixed and the top plate was oscillating back and forth with ranging frequencies to simulate shearing action. The analysis is conducted at 9 different frequencies ranging from 0.159 Hz to 15.92 Hz. The analysis is software controlled, while measured stresses and resulting strains were obtained in terms of complex modulus (G*) and phase angle (δ), which are considered as the most significant parameters to define the rutting (G*/sin δ) and fatigue (G*.sin δ) performance of bitumen binders. The effect of temperature on the performance of bitumen binders was illustrated using isochronal plots, master curves, and rutting performance graphs. G* results were used in the construction of master curves. To represent the results in a single curve known as a master curve, a reference temperature of 64^{o}C was defined and frequencies were shifted relative to this temperature Where RTFO of 39 ± 1 gram placed in the oven on 163 ^{o}C ± 1 in place of 85 minutes for short term during the constructed period of 4-5hrs and PAV of 50 ± 1 gram placed in the oven on 100 ^{o}C ± 1 in place of 20hrs for a long term period of 3-5years and 5-10 years was prepared. And the performance of the modified binders was observed in a range of temperatures (10 ^{o}C-80 ^{o}C) and frequencies (1.5Hz-146Hz), while isochronal plots, master curves, and rutting parameter plots were used in the evaluation of performance characteristics. (Ali et al., 2015). The log-linear approach was adopted in this study using relevant shift factor constants at each test temperature to obtain the best fitting master curve.

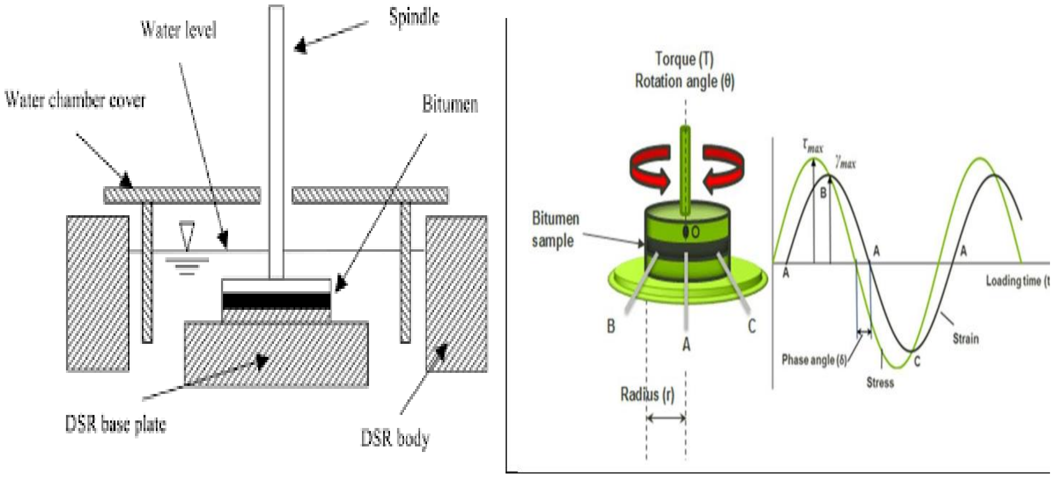

Figure 3.9: Schematic presentation of DSR

CHAPTER 4

RESULTS AND DISCUSSION

4.1 Results of Data-Driven Models

As mentioned, in chapter three the study presented various computational models including MLPNN, ELM, LSSVM, and Stepwise Regression analysis (SWLR) analysis is carried out to predict the G* and δ of polymer nano-composite modified bitumen. For this purpose, all the models MLP, ELM, LSSVM, and Stepwise Regression analysis (SWLR) were developing using MATLAB 9.3 (R2017a), the model input selection was employed concerning correlation analysis. Subsequently, three different ensemble learning approach viz: SAE, WAE, and NNE to improve the overall efficiency with regards to prediction performance. Both the conventional, computational model, and ensemble learning techniques results were evaluated using three different performance criteria viz: determination coefficient (DC), RMSE, and R.

With reference to pre-examination and processing the information, Table 4.1 present factual investigation of the factors associated with the forecast. The measured test information was adequate to cover all the sensible forecast. As per (Elkiran et al., 2019) an extremely high Csx can influence the exhibition of ANN extensively, whereas a small Csx is increasingly suitable for demonstrating. This legitimizes our forecast presentation results particularly for stage edge (δ). Further examination was done utilizing the connection network to quantify the quality and bearing related among the different classes. To the improvement of any prescient model methodologies, assurance of the connection coefficient is significant, because the guiding symbol (+ or -) demonstrates the connection among the classes (Table 4.2). Based on Table 2 (see also Fig. 4.1 and 4.2), the correlation results demonstrated a combination of both negative and positive relationship between the variables. From the correlation analysis, it can be seen that frequency and temperature are more correlated and therefore considered as M1, while in M2 contained the addition of softening point and penetration as shown in Table 4.

Table 4.1: Statistical Analysis of the variables

Variables	X_{mean}	S_x	C_{sx}	X_{min}	X_{max}
Penetration	73.97023	5.106135	-0.00243	66.4	82
Softening point	52.50131	3.504578	-0.84627	46	56
Temperature (^{o}C)	64.14099	12.11252	-0.0092	46	82
Frequency (Hz)	4.359014	5.153004	1.290405	0.159	15.92
|G*| (Pa)	4830.918	12235.1	6.031041	10.86	117800
δ	86.43951	2.816648	-2.13366	69.47	89.08709

Table 4.2: Correlation Analysis between the experimental variables

Variables	Penetration	Softening point	Temperature (^{o}C)	Frequency (Hz)	|G*| (Pa)	δ
Penetration	1					
Softening point	-0.80263	1				
Temperature (^{o}C)	0.005546	0.0039	1			
Frequency (Hz)	0.006705	0.00552	0.02205	1		
|G*| (Pa)	-0.06858	0.158232	-0.39143	0.434764	1	
δ	0.047332	-0.00292	0.624596	-0.50164	-0.66742	1

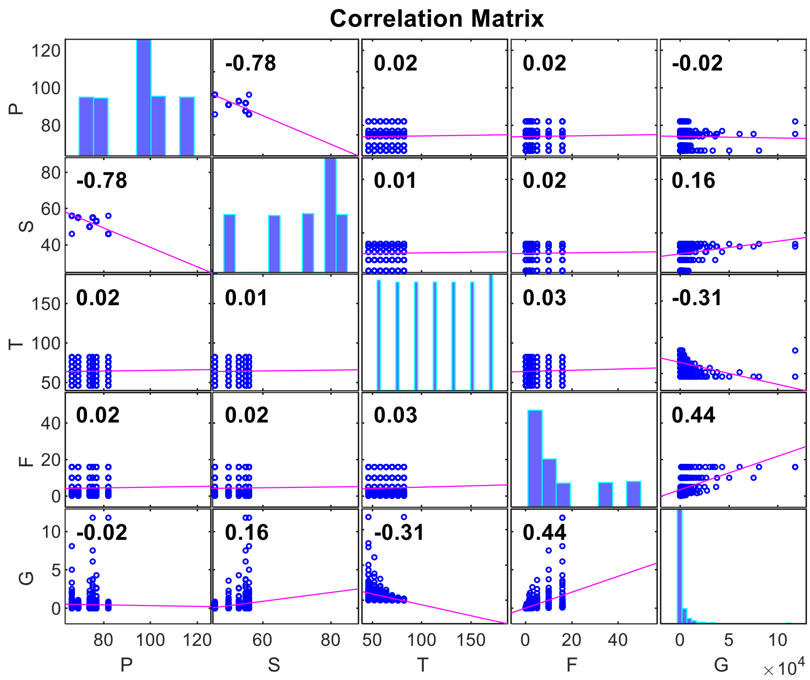

Figure 4.1: Correlation between the experimental parameter for G*

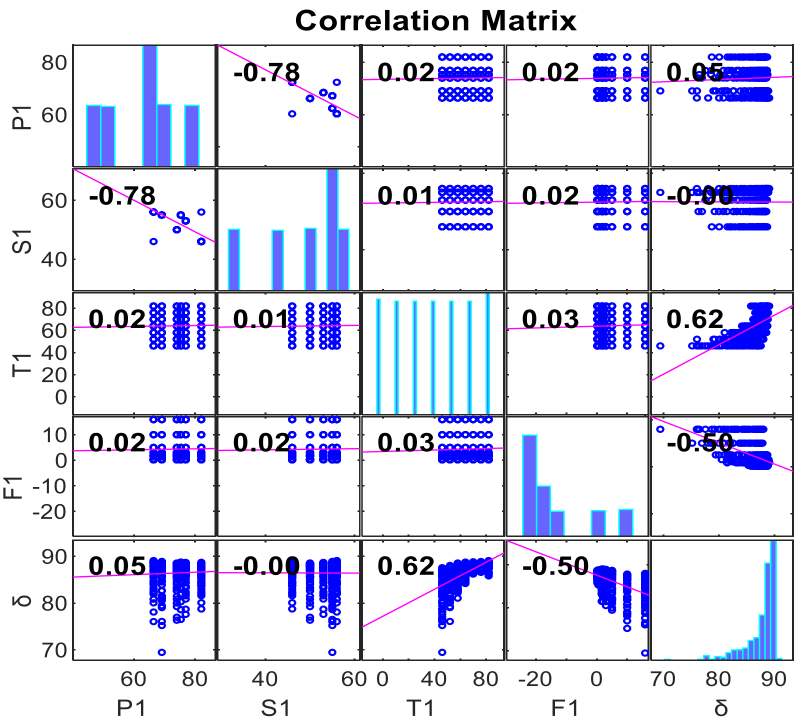

Figure 4.2: Correlation between the experimental parameter for δ

Table 4.3: Input variable combination

Model Type	Model Input combination
MLPNN	M1 (Frequency +Temperature)
	M2 (Frequency +Temperature+ Softening point+ Penetration)
ELM	M1 (Frequency +Temperature)
	M2 (Frequency +Temperature+ Softening point+ Penetration)
LSSVM	M1 (Frequency +Temperature)
	M2 (Frequency +Temperature+ Softening point+ Penetration)
SWLR	M1 (Frequency +Temperature)
	M2 (Frequency +Temperature+ Softening point+ Penetration)
Ensemble	*f* (MLPNN+ELM+LSSVM+SWLR)

4.2 Results of Multi-layer Perceptron Neural Network (MLPNN)

For modeling MLPNN, a total of 381 experimental data were obtained and portioned into training and testing phase. Based two model combination (M1 and M2) the network was obtained as in Fig 4.3 and the tangent sigmoid activation function was employed due to promising ability in various science and engineering research (Nourani et al., 2018).

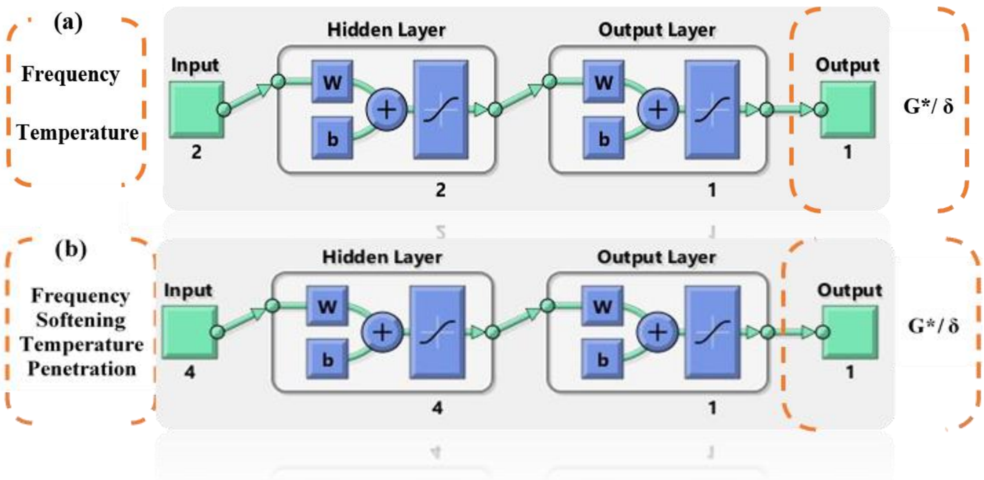

Figure 4.3: Network topology for M1 and M2 model combination

Table 4.4 shows the results performance of MLPNN for modeling the (G*) and (δ) of polymer nano-composite modified bitumen. From the table, it can be seen that MLPNN us capable of predicting (G*) using a model combination of M2 that contained four input combination with the high accuracy in term of DC.

Table 4.4: Performance results of MLPNN model for (G*) and (δ)

			Training			Testing		
	Outputs	Model	DC	RMSE	R	DC	RMSE	R
	(G*)	M1	0.6239	0.0695	0.7899	0.6062	0.0162	0.7786
MLPNN		M2	0.9525	0.0238	0.9760	0.9645	0.0101	0.9821
	(δ)	M1	0.9957	0.0442	0.9978	0.9895	0.0260	0.9948
		M2	0.9969	0.0391	0.9984	0.9971	0.0229	0.9985

Similarly, the results demonstrated the ability of the MLPNN model in modeling and predicting (δ) with both the model combination M1 and M2. Which is justified by looking all the evaluation indexes in both calibration and verification. However, the computed correlation using formula and software are approximately the same. The error training function graph for both M1 and M2 ((G*) and (δ)) can be presented in Fig. 4.4.

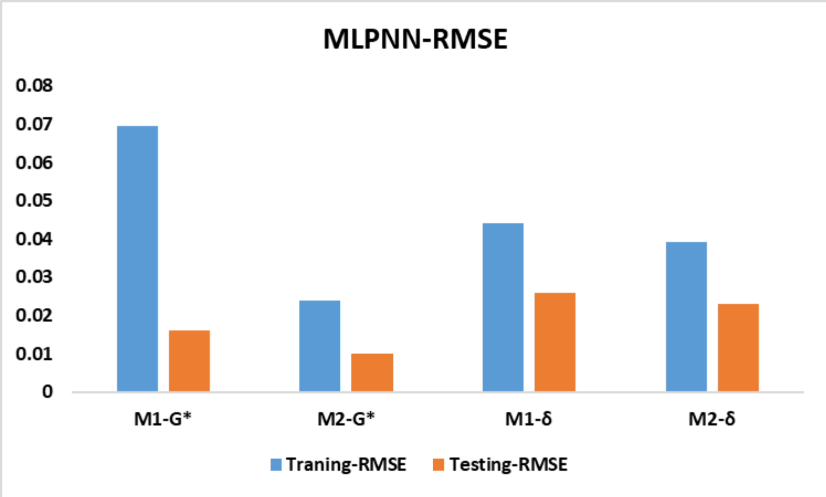

Figure 4.4: Error function of MLPNN for (a) M1 and (b)M2 for (G*)

Further examination of the experimental versus predicted results can be shown in the performance graph obtained from Matlab software (Fig. 4.4). This plot was obtained based on the mean square error calculated by considering the observed and computed values. According to the plots, it can be justified that for the prediction of the (G*) and (δ) of polymer nano-composite modified bitumen, M2-MLPNN model outperformed models M1-MLPNN and can be served as the reliable prediction model. Meanwhile, the outcomes also showed that using four combinations of variable as in M2 will increased the performance efficiency and thereby recommended to includes the softening point and penetration particularly for modeling complex modulus but in case of angle phase both M1 and M2 can serve the prediction expectation. Fig. 4.4 also shows the scatter plot of the best models for predicting and modeling the predicted outcomes of polymer nano-composite modified bitumen.

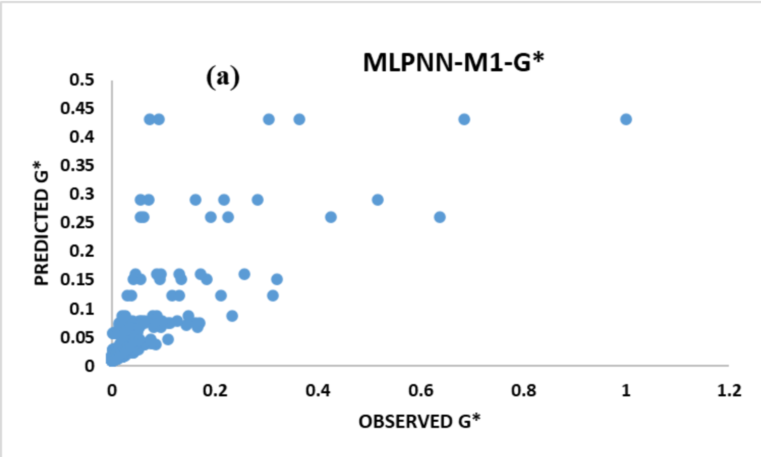
MLPNN-M1-G*
(a)
PREDICTED G*
OBSERVED G*
0.5
0.45
0.4
0.35
0.3
0.25
0.2
0.15
0.1
0.05
0
0
0.2
0.4
0.6
0.8
1
1.2

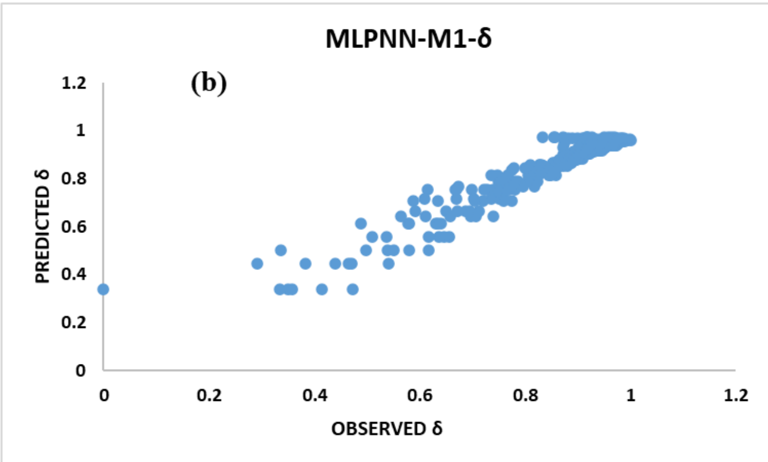
MLPNN-M1-δ
(b)
PREDICTED δ
OBSERVED δ
1.2
1
0.8
0.6
0.4
0.2
0
0
0.2
0.4
0.6
0.8
1
1.2

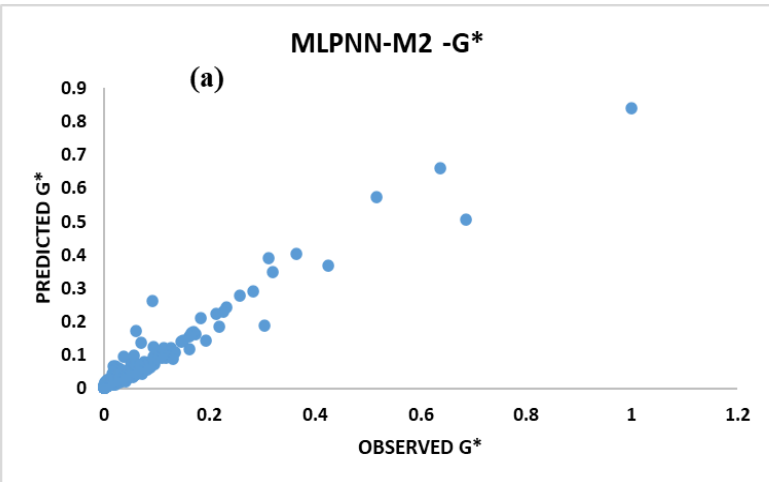
MLPNN-M2 -G*
(a)
PREDICTED G*
OBSERVED G*
0.9
0.8
0.7
0.6
0.5
0.4
0.3
0.2
0.1
0
0
0.2
0.4
0.6
0.8
1
1.2

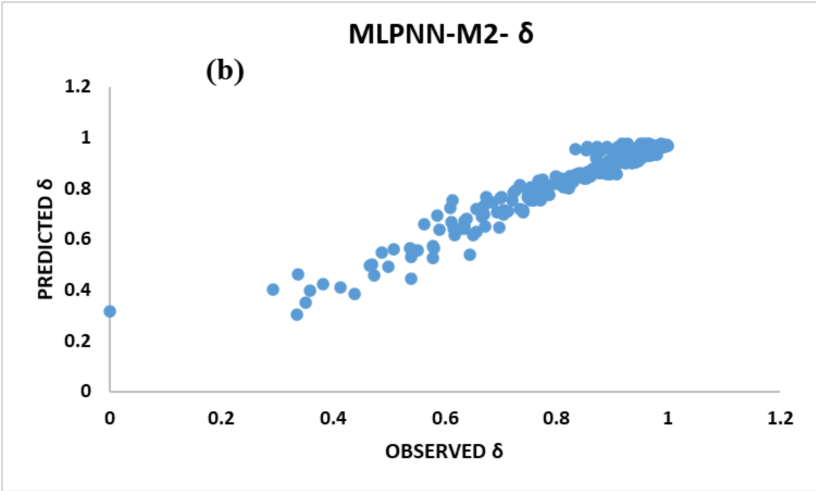

Figure 4.5: Scatter plots showing the experimental versus predicted for (a) G* (b) (δ)

4.3 Extreme Learning Machine (ELM)

For the simulation using ELM, 381 data points were obtained experimentally, which are further classified into calibration and verification stage. Based on the input parameters two models (M1 and M2) combination. According to table 4.5, the predictive performance results of ELM for the simulation of complex modulus was demonstrated (G*) and phase angle (δ) of polymer nano-composite modified bitumen. It can be observed from the table that ELM has the ability to model each complex modulus was demonstrated (G*) and phase angle (δ) of polymer nano-composite modified bitumen. Even though for modelling G* in M1 shows a weak prediction as compared with the M1 simulation of δ having a DC value of 0.6662 and 0.9953 respectively. Overall, M2 with four input variables proved to have shown the highest performance for modelling both predicted outcomes of polymer nano-composite modified bitumen in both training and testing stages using the ELM model as shown in table 4.5

Additional inspection of the experimental versus predicted results for ELM can be shown in the performance graph obtained from Matlab software (Fig. 4.6). This plot was obtained based on point by point calculated by considering the observed and computed values. According to the plots, it can be justified that for the prediction of the predicted outcomes of polymer nano-composite modified bitumen, M2-ELM model outperformed models M1-

ELM and can serve as the reliable prediction model. Meanwhile, the outcomes also showed that using four combinations of variable as in M2 will increase the performance efficiency and thereby recommended to includes the softening point and penetration particularly for modeling complex modulus but in case of angle phase both M1 and M2 can be served the prediction expectation. Table. 4.5 also shows model combination of predicted outcomes of polymer nano-composite modified bitumen.

Table 4.5: Performance results of ELM model for (G*) and (δ)

			Training			Testing		
	Outputs	Model	DC	RMSE	R	DC	RMSE	R
ELM	(G*)	M1	0.6549	0.0645	0.8093	0.6662	0.0112	0.8162
		M2	0.9725	0.0188	0.9862	0.9745	0.0051	0.9872
	(δ)	M1	0.9887	0.0392	0.9943	0.9913	0.0210	0.9957
		M2	0.9900	0.0341	0.9950	0.9921	0.0179	0.9960

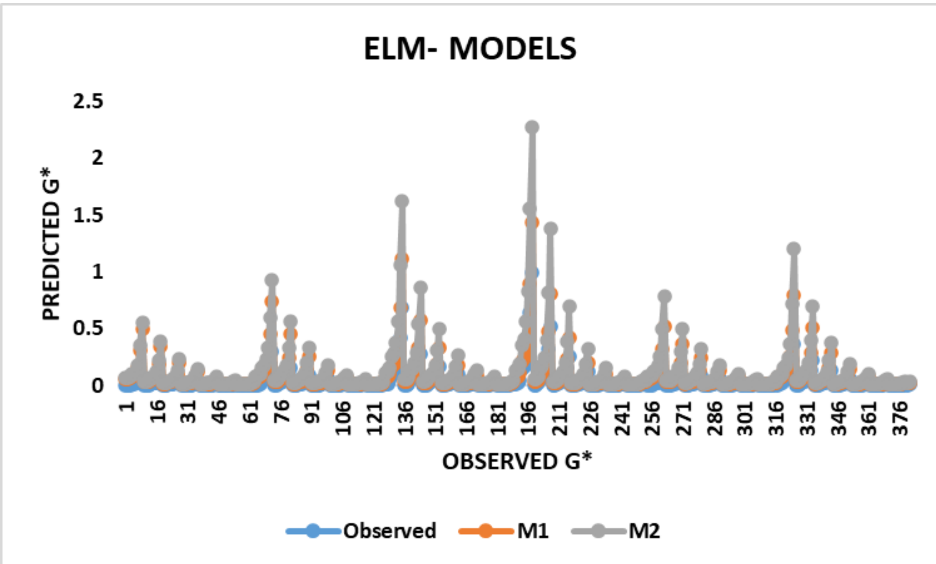

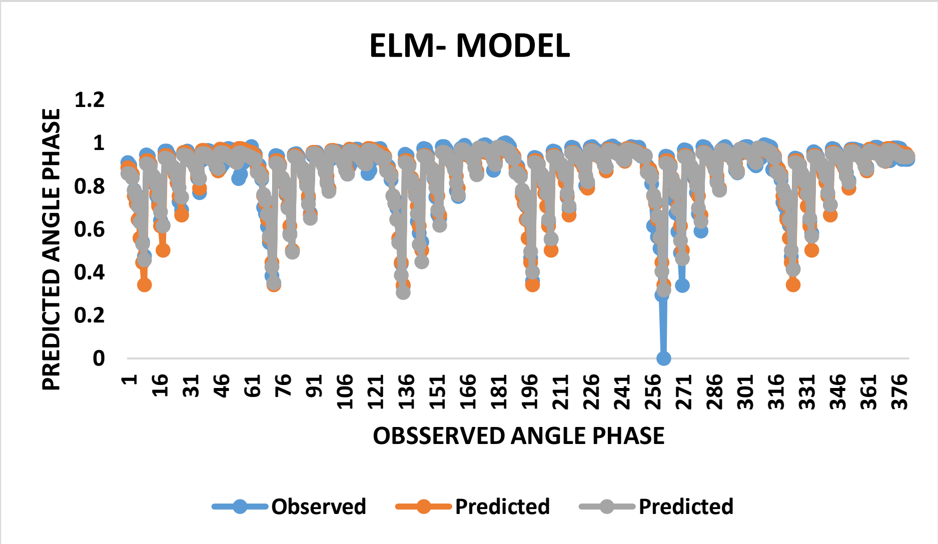

Figure 4.6: Point to point plots of the experimental vs predicted value for (a) G* (b) (δ)

4.4 Results of Least Square Support Vector Machine (LSSVM)

However, the results in Table 4.6 shows the performance efficiency of LSSVM for the prediction of G* and (δ) of nano-composite modified bitumen. From the results, it can be seen that the SVM model, as MLPNN was trained using two different models M1 and M2. Among the combination models of SVM, M2 has the highest values of DC and the lowest values of RMSE both in training and testing data, therefore emerged the best models. Fig 4.6 shows radar between the experimental and computed values for the best model of G* and (δ) (M2).

Table 4.6: Performance results of LSSVM model for (G*) and (δ)

	Outputs	Models	Training			Testing		
			DC	RMSE	R	DC	RMSE	R
LSSVM	(G*)	M1	0.4873	0.0321	0.6981	0.4464	0.0117	0.6681
		M2	0.6339	0.0291	0.7962	0.5010	0.0107	0.7078
	(δ)	M1	0.7096	0.0387	0.8424	0.5864	0.0245	0.7651
		M2	0.7149	0.0380	0.8455	0.5876	0.0242	0.7666

From Table 4.6 can be concluded that the LSSVM model is not capable of predicting both G* and (δ) of nano-composite modified bitumen. This is proved by considering the valued of DC, RMSE and R coefficients. It is worth mentioning that the higher value of DC and R the better the performance analysis results and vice versa. On the other hand, the lower the value of RMSE the better the prediction accuracy. Even though the values of RMSE are low but the goodness of fit in all the model combination is low and there marked the results unreliable. The results indicated that the LSSVM model need to be finetune using some parameters or there is a need for introducing an optimization approach to improve the results of LSSVM model before being put into application.

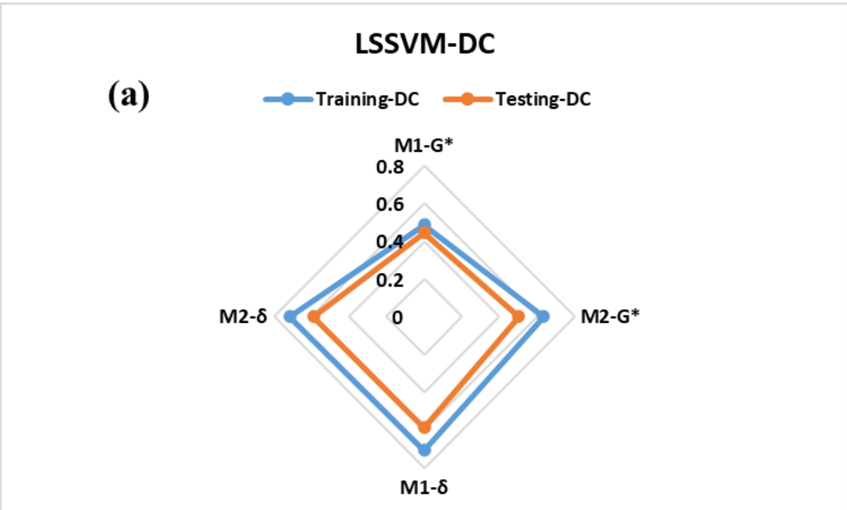

Figure 4.7: Radar charts of the experimental vs predicted value for (a) DC (b) R

4.5 Results of Stepwise Regression analysis (SWLR)

A the classical SWLR method was also determined employing two different input combinations as stated above. For the SWLR Model, the analysis was carried out in SPSS software (2018) and the performance results were computed in Microsoft excel as can be seen in Table 4.7. From Table 4.7, it can be observed that M2 outperformed M2 in term of DC, RMSE and R. The linear model was employed to investigate the linear relationship with the materials. The results also explained that the SWLR model is not fit for the prediction of G* and (δ) of nano-composite modified bitumen. From the result we can conclude that SWLR is no a reliable model for both the two combinations (see, Fig. 4.7). Fig 4.8 shows point to point plots between the experimental and computed values for the best model of G* and (δ) (M2).

Table 4.7: Performance results of SWLR model for (G*) and (δ)

			Training			Testing		
	Outputs	Models	DC	RMSE	R	DC	RMSE	R
SWLR	(G*)	M1	0.3448	0.0804	0.5872	0.3223	0.0265	0.5677
		M2	0.3889	0.0776	0.6236	0.3714	0.0240	0.6094
	(δ)	M1	0.6608	0.0720	0.8129	0.6517	0.0681	0.8073
		M2	0.6711	0.0334	0.8192	0.6595	0.0455	0.8121

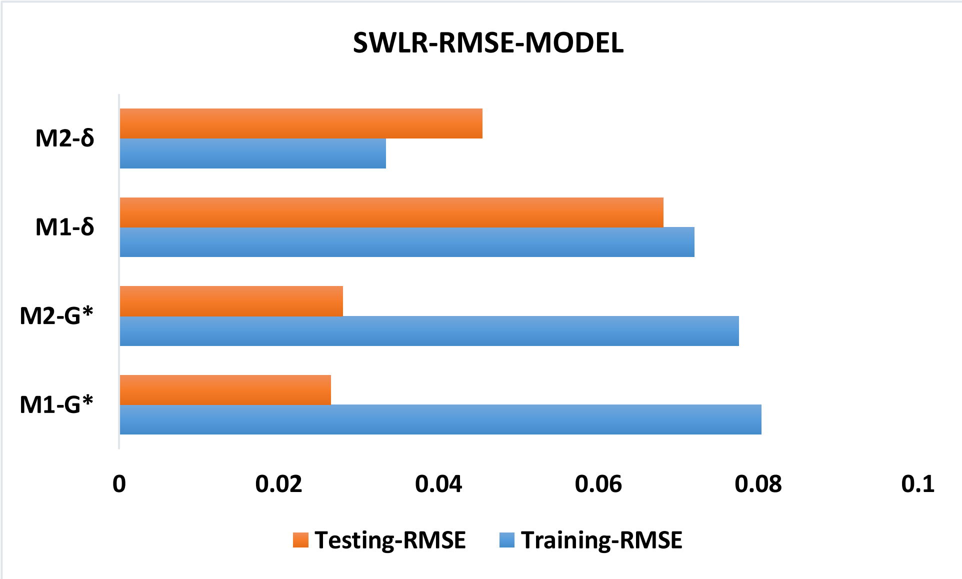

Figure 4.8: Error function of SWLR for (a) M1 and (b)M2 for (G*)

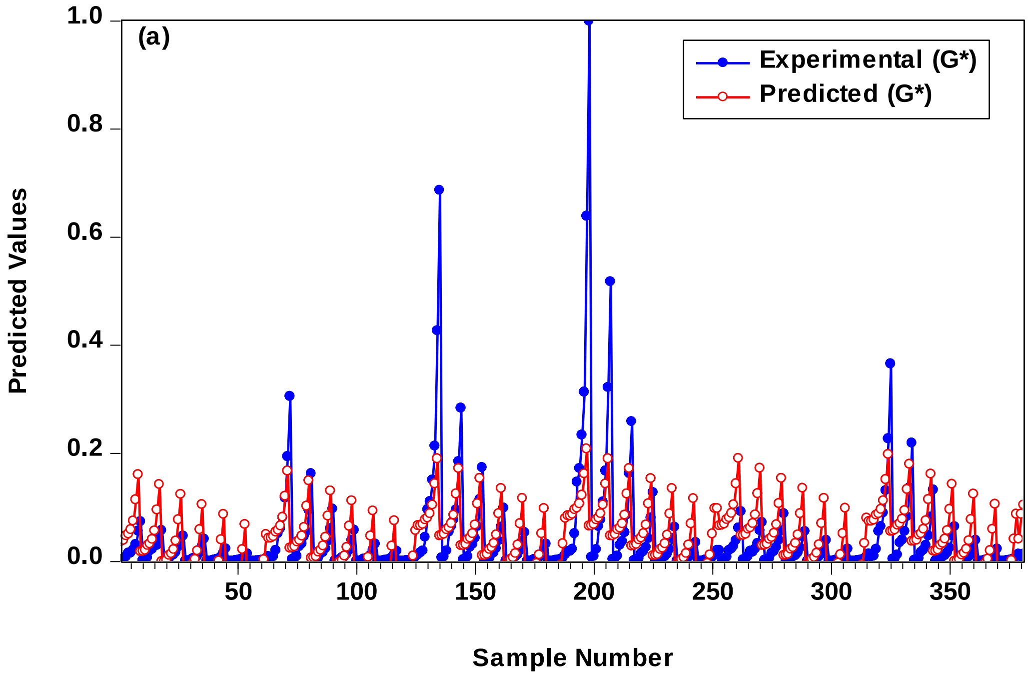

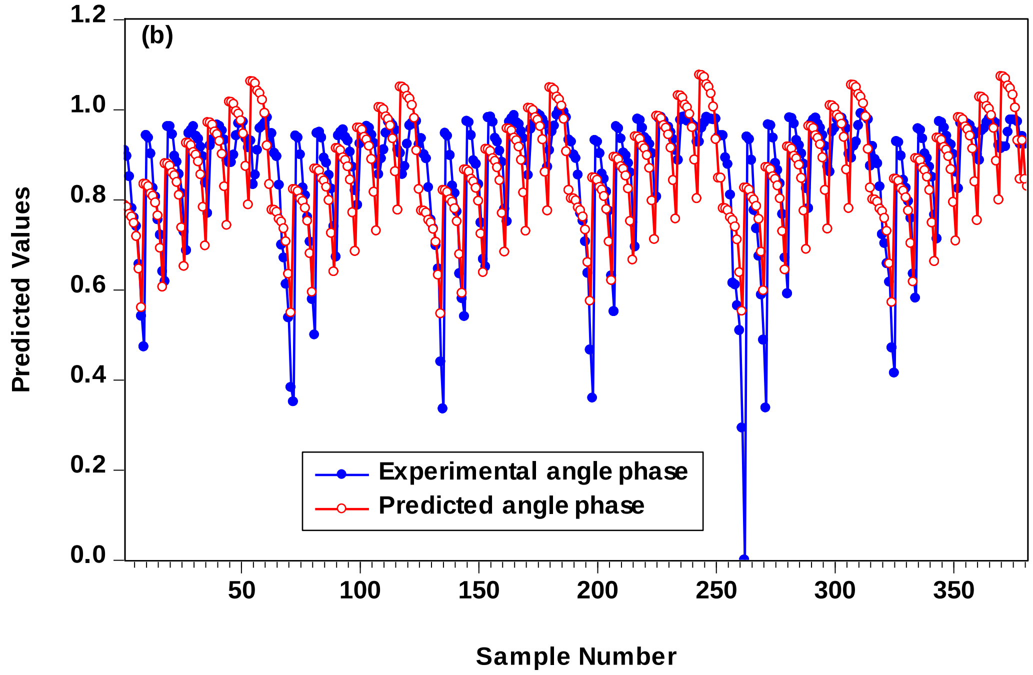

Figure 4.9: Point to point plots of the experimental vs predicted value for (a) G* (b) (δ)

4.6 Ensemble Learning Results

Based on the predictive performance results of the ensemble machine learning techniques, it is indicated that all the three employed ensemble methods have the ability to model both predicted outcomes of polymer nano-composite modified bitumen in both training and testing stages. According to table 4.8 neural network ensemble (NNE) proved to have shown higher performance efficiency than WAE and SAE in both calibration and verification phases respectively, by employing the three performance indices; DC, RMSE and R.

Table 4.8: Performance results of three types of ensemble model for (G*) and (δ)

		Training			Testing		
Outputs	Model	DC	RMSE	R	DC	RMSE	R
G*	NNE	0.9925	0.0128	0.9962	0.9975	0.0090	0.9987
δ	NNE	0.9989	0.0332	0.9994	0.9973	0.0150	0.9987
G*	WAE	0.7676	0.0585	0.8761	0.7686	0.0052	0.8767
δ	WAE	0.9980	0.0281	0.9990	0.9969	0.0119	0.9985
G*	SAE	0.8549	0.0659	0.9246	0.8456	0.0099	0.9196
δ	SAE	0.9979	0.0481	0.9989	0.9961	0.0204	0.9980

A radar plot can be employed for a better comparison of the three ensemble machine learning techniques by employing both the correlation coefficient (R) and determination co-efficient (DC). The DC and R values for both the training and testing stages are shown for the modelling of both predicted outcomes of polymer nano-composite modified bitumen (See Fig. 4.9).

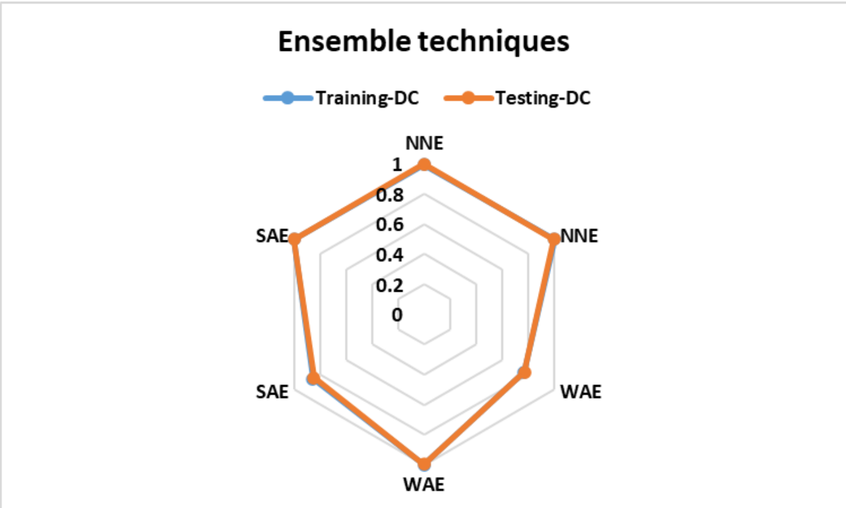

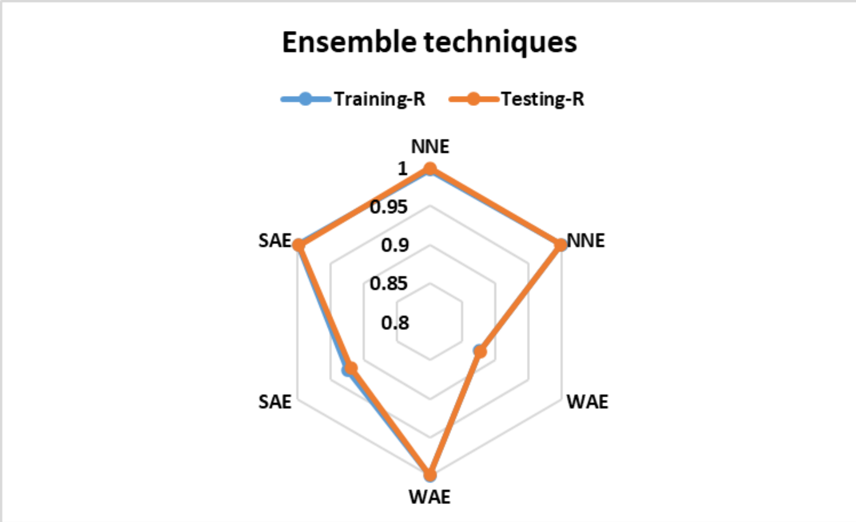

Figure 4.10: Radar charts of the experimental vs predicted value for (a) DC (b) R

The predictive performance of the ensemble machine learning technique can equally be demonstrated in terms of RMSE using a bar chart (see Fig. 4.10). Based on the chart, it can be observed that NNE having lower values of RMSE has outperformed the other two techniques, and this is in line with table 4.8.

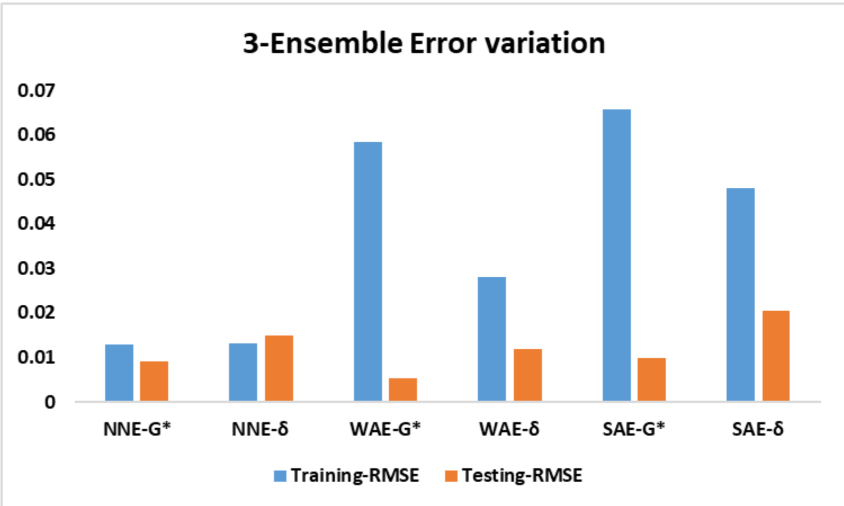

Figure 4.11: Error function of the ensemble for RMSE

CHAPTER 5

CONCLUSIONS AND RECOMMENDATION

5.1 Conclusion

The study employed four data driven models including MLP, ELM, LSSVM, and Stepwise Regression analysis (SWLR) analysis is carried out to predict the complex modulus (G*) and phase angle (δ) of polymer nano-composite modified bitumen. For this purpose, all the models MLP, ELM, LSVM, and Stepwise Regression analysis (SWLR) were developed using MATLAB 9.3 (R2017a), the model input selection was done out based on the correlation analysis Subsequently, three different ensemble learning approach viz: SAE, WAE, and NNE to improve the overall efficiency with regards to prediction performance. Both the conventional, computational model, and ensemble learning techniques results were evaluated using three different performance criteria viz: determination coefficient (DC), root mean square error (RMSE), and correlation coefficient (R). The computation models (MLPNN, ELM, and LSSVM) shows better prediction performance than the conventional SWLR model with M2- ELM outperformed all the single computational models by producing complex modulus G* values of DC=0.9745, RMSE=0.0051 and R= 0.9872 while M2-MLPNN is better than all the models with respect to the prediction of phase angle δ with values of DC= 0.9971, RMSE=0.0229 and R= 0.9985. It is indicated that all three employed ensemble methods have the ability to model both G* and δ. According to prediction results NNE proved to have shown higher performance efficiency than WAE and SAE in both the calibration and verification phases respectively, by employing the three performance indices; DC, RMSE and R.

The physical properties, stiffness (G*) and rutting resistance of unmodified, polymer modified and polymer nano-composite materials of Nano copper and Nano calcium modified at 3% and 5% concentrations to the weight of bitumen were investigated under a range of temperatures and frequencies using DSR. According to the test results and analytical models' performance evaluation, the following conclusions can be drawn:

I. Based on the predictive performance results of the ensemble machine learning techniques, it is indicated that all the three employed ensemble methods have the ability to model both complex modulus (G*) and phase angle (δ) of polymer nano-composite modified bitumen in both training and testing stages. According to table 4.8 neural network ensemble (NNE) proved to have shown higher performance efficiency than WAE and SAE in both the calibration and verification phases respectively, by employing the three performance indices; DC, RMSE and

II. Based on the results ELM model it can be justified that for the prediction of the complex modulus (G*) and phase angle (δ) of polymer nano-composite modified bitumen, M2-ELM model outperformed models M1-ELM and can be served as the reliable prediction model. Meanwhile, the outcomes also showed that using four combinations of variable as in M2 will increase the performance efficiency and thereby recommended to includes the softening point and penetration particularly for modeling complex modulus but in case of angle phase both M1 and M2 can be served the prediction expectation

III. MLP and SVM model is also capable of predicting both G* and (δ) of nano-composite modified bitumen. This is proved by considering the valued of DC, RMSE and R coefficients. It is worth mentioning that the higher value of DC and R the better the performance analysis results and vice versa.

IV. The linear model (SWLR) was employed to investigate the linear relationship with the materials. The results also explained that the SWLR model is not fit for the prediction of G* and (δ) of nano-composite modified bitumen. From the result we can conclude that SWLR is not a reliable model for both the two combined.

V. Maximum enhancement in G* and (δ) was observed to be slightly above 1.00 E+05 Pa with 3% ASA-Nano calcium modified binder.Increasing the polymer nano-composite material content enhanced the properties of the asphalt binder up to 3% concentration. However further use of modifier at 5% concentration to the weight of bitumen resulted in lower G* and rutting resistance, which is considered to be due to incompatibility of bitumen with the modifier. It was observed that 5% ASA modified and 5% ASA-Nano calcium and 5% ASA-Nano copper modified blends demonstrated an almost equal enhancement in the rheological properties of asphalt binder.

5.2 Recommendation

According to a study conducted by Ali et al., (2015) the ASA modified bitumen with base 60/80 grade provided higher G* and (δ) values and therefore, it is significant that among the types of modifier materials, the penetration grade of base bitumen significantly influences the performance of asphalt binders. However, based on data have driven models, it is also suggested that more algorithms and optimization methods should be introduced and practiced in order to predict the complex modulus (G*) and phase angle (δ) of polymer nano-composite modified bitumen. As such, genetic algorithms, particle swam optimization, deep learning algorithms should be used in future studies.

REFERENCES

Abba, S. I., Pham, Q. B., Usman, A. G., Linh, N. T. T., Aliyu, D. S., Nguyen, Q., & Bach, Q. V. (2020b). Emerging evolutionary algorithm integrated with kernel principal component analysis for modeling the performance of a water treatment plant. *Journal of Water Process Engineering*, *33*(October 2019), 101081. https://doi.org/10.1016/j.jwpe.2019.101081

Abba, S I, Jasim, S., Sh, S., Salih, S. Q., & Abdulkadir, R. A. (2020). Evolutionary computational intelligence algorithm coupled with self-tuning predictive model for water quality index determination. *Journal of Hydrology*, *587*(March), 124974. https://doi.org/10.1016/j.jhydrol.2020.124974

Abdelrahman, M., Katti, D. R., Ghavibazoo, A., Upadhyay, H. B., & Katti, K. S. (2014). Engineering physical properties of asphalt binders through nanoclay–asphalt interactions. *Journal of Materials in Civil Engineering, 26*(12), 04014099.

Abedali, A. H. (2015). Predicting complex shear modulus using artificial neural networks. *Journal of Civil Engineering and Construction Technology*, *6*(3), 15-26.

Adlinge, S. S., & Gupta, A. (2013). Pavement deterioration and its causes. *International Journal of Innovative Research and Development*, *2*(4), 437-450.

Airey, G. D. (2003). Rheological properties of styrene butadiene styrene polymer modified road bitumens☆. *Fuel, 82*(14), 1709-1719.

Al-Khateeb, G. G., & Al-Akhras, N. M. (2011). Properties of Portland cement-modified asphalt binder using Superpave tests. *Construction and Building Materials, 25*(2), 926-932.

Al-Mansob, R. A., Ismail, A., Alduri, A. N., Azhari, C. H., Karim, M. R., & Yusoff, N. I. M. (2014). Physical and rheological properties of epoxidized natural rubber modified bitumens. *Construction and Building Materials*, *63*, 242-248.

Ali, S. I. A., Ismail, A., Karim, M. R., Yusoff, N. I. M., Al-Mansob, R. A., & Aburkaba, E. (2017). Performance evaluation of Al2O3 nanoparticle-modified asphalt binder. *Road Materials and Pavement Design, 18*(6), 1251-1268.

Amirkhanian, A. N., Xiao, F., & Amirkhanian, S. N. (2010). Evaluation of high temperature rheological characteristics of asphalt binder with carbon nano particles. *Journal of Testing and Evaluation, 39*(4), 583-591.

Abdulkadir, R. A., Ali, S. I. A., Abba, S. I., & Esmaili, P. (2020). Forecasting of daily rainfall at Ercan Airport Northern Cyprus: a comparison of linear and non-linear models. *Desalination and Water Treatment*, *177*(May 2019), 297–305. https://doi.org/10.5004/dwt.2020.25321

Abdullahi, H. U., Usman, A. G., & Abba, S. I. (2020). Modelling the Absorbance of a Bioactive Compound in HPLC Method using Artificial Neural Network and Multilinear Regression Methods, *6*(2), 362–371.

Aqil, M., Kita, I., Yano, A., & Nishiyama, S. (2007). Analysis and prediction of flow from local source in a river basin using a Neuro-fuzzy modeling tool. *Journal of environmental management*, *85*(1), 215-223.

Asadi, S., Hassan, M., Nadiri, A., & Dylla, H. (2014). Artificial intelligence modeling to evaluate field performance of photocatalytic asphalt pavement for ambient air purification. *Environmental Science and Pollution Research, 21*(14), 8847-8857.

Bala, N., Napiah, M., & Kamaruddin, I. (2018). Nanosilica composite asphalt mixtures performance-based design and optimisation using response surface methodology. *International Journal of Pavement Engineering*, 1-12.

Baldo, N., Manthos, E., & Pasetto, M. (2018). Analysis of the Mechanical Behaviour of Asphalt Concretes Using Artificial Neural Networks. *Advances in Civil Engineering, 2018*.

Becker, Y., & Méndez, M. P. (2001). and Yajaira Rodríguez. *VISION TECNOLOGICA*, *9*(1), 39.

Bradshaw, J. M. (1997). An introduction to software agents. *Software agents*, *5*, 3-46.

Brasileiro, L., Moreno-Navarro, F., Tauste-Martínez, R., Matos, J., & Rubio-Gámez, M. d.

C. (2019). Reclaimed Polymers as Asphalt Binder Modifiers for More Sustainable

Roads: A Review. *Sustainability, 11*(3), 646.

Brown, S., & Needham, D. (2000). A study of cement modified bitumen emulsion mixtures. *Asphalt Paving Technology, 69*, 92-121.

Burger, A., Van de Ven, M., Jenkins, K., & Muller, J. (2001). Rheology of polymer modified bitumen: a comparative study of three binders and three binder/filter systems. *SATC 2001*.

Cuadri, A., Partal, P., Navarro, F., García-Morales, M., & Gallegos, C. (2011a). Bitumen chemical modification by thiourea dioxide. *Fuel, 90*(6), 2294-2300.

Cuadri, A., Partal, P., Navarro, F., García-Morales, M., & Gallegos, C. (2011b). Influence of processing temperature on the modification route and rheological properties of thiourea dioxide-modified bitumen. *Energy & Fuels, 25*(9), 4055-4062.

Cüneyt Aydin, A., Tortum, A., & Yavuz, M. (2006). Prediction of concrete elastic modulus using adaptive neuro-fuzzy inference system. *Civil Engineering and Environmental Systems, 23*(4), 295-309.

Dasgupta, D. (1993). An Overview of Artificial Immune Systems and Their Applications. *Springer-Verlag Berlin Heidelberg*.

El-Badawy, S., Abd El-Hakim, R., & Awed, A. (2018). Comparing Artificial Neural Networks with Regression Models for Hot-Mix Asphalt Dynamic Modulus Prediction. *Journal of Materials in Civil Engineering, 30*(7), 04018128.

El-Basyouny, M. M., & Witczak, M. (2005). Calibration of alligator fatigue cracking model for 2002 design guide. *Transportation research record, 1919*(1), 76-86.

Ezzat, H., El-Badawy, S., Gabr, A., Zaki, E.-S. I., & Breakah, T. (2016). Evaluation of asphalt binders modified with nanoclay and nanosilica. *Procedia engineering, 143*, 1260-1267.

Elkiran, G., Nourani, V., Abba, S. I., & Abdullahi, J. (2018). Artificial intelligence-based approaches for multi-station modelling of dissolve oxygen in river. *Global Journal of Environmental Science and Management, 4*(4), 439–450. https://doi.org/10.22034/gjesm.2018.04.005

Elkiran, Gozen, Nourani, V., & Abba, S. I. (2019). Multi-step ahead modelling of river water quality parameters using ensemble artificial intelligence-based approach. *Journal of Hydrology*, *577*, 123962. https://doi.org/10.1016/j.jhydrol.2019.123962

Fang, C., Yu, R., Liu, S., & Li, Y. (2013). Nanomaterials applied in asphalt modification: a review. *Journal of Materials Science & Technology, 29*(7), 589-594.

Firouzinia, M., & Shafabakhsh, G. (2018). Investigation of the effect of nano-silica on thermal sensitivity of HMA using artificial neural network. *Construction and Building Materials, 170*, 527-536.

Golestani, B., Nam, B. H., Nejad, F. M., & Fallah, S. (2015). Nanoclay application to asphalt concrete: Characterization of polymer and linear nanocomposite-modified asphalt binder and mixture. *Construction and Building Materials, 91,* 32-38.

Golzar, K., Jalali-Arani, A., & Nematollahi, M. (2012). Statistical investigation on physical–mechanical properties of base and polymer modified bitumen using Artificial Neural Network. *Construction and Building Materials, 37*, 822-831.

Gaya, M. S., Abba, S. I., Abdu, A. M., & Tukur, A. I. (2020). Estimation of water quality index using artificial intelligence approaches and multi-linear regression, *9*(1), 126–134. https://doi.org/10.11591/ijai.v9.i1.pp126-1A34

Hadi, S. J., Abba, S. I., Sammen, S. S., Salih, S. Q., Al-Ansari, N., & Yaseen, Z. M. (2019). Non-Linear Input Variable Selection Approach Integrated With Non-Tuned Data Intelligence Model for Streamflow Pattern Simulation. *IEEE Access*, *7*, 141533–141548. https://doi.org/10.1109/access.2019.2943515

Habib, N. Z., Kamaruddin, I., Napiah, M., & Isa, M. T. (2011). Rheological properties of polyethylene and polypropylene modified bitumen. *International Journal Civil and Environmental Engineering, 3*(2), 96-100.

Jahromi, S. G., & Khodaii, A. (2009). Effects of nanoclay on rheological properties of bitumen binder. *Construction and Building Materials, 23*(8), 2894-2904.

Jang, J.-S. R., Sun, C.-T., Mizutani, E., & Ho, Y. (1998). Neuro-fuzzy and soft computing-a computational approach to learning and machine intelligence. *Proceedings of* *the IEEE, 86*(3), 600-603.

Johanneck, L., & Khazanovich, L. (2010). Comprehensive Evaluation of Effect of Climate in Mechanistic–Empirical Pavement Design GuidePredictions. *Transportation research record, 2170*(1), 45-55.

Kar, S., Das, S., & Ghosh, P. K. (2014). Applications of neuro fuzzy systems: A brief review and future outline. *Applied Soft Computing, 15*, 243-259.

Khademi, F., Jamal, S. M., Deshpande, N., & Londhe, S. (2016). Predicting strength of recycled aggregate concrete using artificial neural network, adaptive neuro-fuzzy inference system and multiple linear regression. *International Journal of Sustainable Built Environment, 5*(2), 355-369.

Kim, Y. R. (2008). *Modeling of asphalt concrete*.

Kishchynskyi, S., Nagaychuk, V., & Bezuglyi, A. (2016). Improving quality and durability of bitumen and asphalt concrete by modification using recycled polyethylene based polymer composition. *Procedia engineering, 143*, 119-127.

Koch, C., Jog, G. M., & Brilakis, I. (2012). Automated pothole distress assessment using asphalt pavement video data. *Journal of Computing in Civil Engineering, 27*(4), 370-378.

Kok, B. V., Yilmaz, M., Sengoz, B., Sengur, A., & Avci, E. (2010). Investigation of complex modulus of base and SBS modified bitumen with artificial neural networks. *Expert Systems with Applications, 37*(12), 7775-7780.

Lamperti, R. (2011). *Rheological and energetic characterization of wax-modified asphalt binders.*

Liu, J., Yan, K., Liu, J., & Zhao, X. (2018). Using artificial neural networks to predict the dynamic modulus of asphalt mixtures containing recycled asphalt shingles. *Journal of Materials in Civil Engineering, 30*(4), 04018051.

Loeber, L., Muller, G., Morel, J., & Sutton, O. (1998). Bitumen in colloid science: a chemical, structural and rheological approach. *Fuel, 77*(13), 1443-1450.

Mirzahosseini, M., Najjar, Y., Alavi, A. H., & Gandomi, A. H. (2013). *ANN-Based prediction model for rutting propensity of asphalt mixtures.* Paper presented at the 92nd Annual Meeting of Transportation Research Board, Washington DC, USA.

Mochinaga, H., Onozuka, S., Kono, F., Ogawa, T., Takahashi, A., & Torigoe, T. (2006). *Properties of Oil sands and Bitumen in Athabasca.* Paper presented at the The Canadian Society of Exploration Geologists CSPG–CSEG–CWLS Convention.

Mohammadi, K., Shamshirband, S., Tong, C. W., Arif, M., Petković, D., & Ch, S. (2015). A new hybrid support vector machine–wavelet transform approach for estimation of horizontal global solar radiation. *Energy Conversion and Management, 92*, 162- 171.

Naderpour, H., & Mirrashid, M. (2018). An innovative approach for compressive strength estimation of mortars having calcium inosilicate minerals. *Journal of Building Engineering, 19*, 205-215.

Ozturk, H. I., Saglik, A., Demir, B., & Gungor, A. (2016). *An artificial neural network base prediction model and sensitivity analysis for marshall mix design.* Paper presented at the Proceedings of the 6th Eurasphalt & Eurobitume Congress, Prague, Czech Republic.

Parmar, K. S., & Bhardwaj, R. (2015). River water prediction modeling using neural networks, fuzzy and wavelet coupled model. *Water resources management, 29*(1), 17-33.

Read, J., & Whiteoak, D. (2003). *The shell bitumen handbook*: Thomas Telford. Robinson, H. (2005). *Polymers in asphalt* (Vol. 15): iSmithers Rapra Publishing.

Rumelhart, D. E., Hinton, G. E., & Williams, R. J. (1985). *Learning internal representations by error propagation*. Retrieved from

Sabadra, V. (2017). Use of Polymer Modified Bitumen in Road Construction. *International Research Journal of Engineering and Technology, 04*(12), 799-801.

Saltan, M., Terzi, S., & Karahancer, S. (2018). Performance analysis of nano modified bitumen and hot mix asphalt. *Construction and Building Materials, 173*, 228-237.

Sarsam, S. I., & Lafta, I. M. (2014). Assessment of Modified-Asphalt Cement Properties. *Journal of Engineering, 20*(6), 1-14.

Sengoz, B., & Isikyakar, G. (2008). Evaluation of the properties and microstructure of SBS and EVA polymer modified bitumen. *Construction and Building Materials, 22*(9), 1897-1905.

Sola, J., & Sevilla, J. (1997). Importance of input data normalization for the application of neural networks to complex industrial problems. *IEEE Transactions on nuclear science, 44*(3), 1464-1468.

Specht, L. P., Khatchatourian, O., Brito, L. A. T., & Ceratti, J. A. P. (2007). Modeling of asphalt-rubber rotational viscosity by statistical analysis and neural networks. *Materials Research*, *10*(1), 69-74.

Speight, J. G. (2015). *Asphalt materials science and technology*: Butterworth-Heinemann.

Talpur, N., Salleh, M. N. M., & Hussain, K. (2017). *An investigation of membership functions on performance of ANFIS for solving classification problems.* Paper presented at the IOP Conference Series: Materials Science and Engineering.

Tapkın, S., Çevik, A., & Uşar, Ü. (2009). Accumulated strain prediction of polypropylene modified marshall specimens in repeated creep test using artificial neural networks. *Expert Systems with Applications, 36*(8), 11186-11197.

Tapkın, S., Çevik, A., & Uşar, Ü. (2010). Prediction of Marshall test results for polypropylene modified dense bituminous mixtures using neural networks. *Expert Systems with Applications, 37*(6), 4660-4670.

User's, F. L. T. T. Guide© COPYRIGHT 1995–2012 The MathWorks: Inc.

Venudharan, V., & Biligiri, K. P. (2017). Heuristic principles to predict the effect of crumb rubber gradation on asphalt binder rutting performance. *Journal of Materials in Civil Engineering, 29*(8), 04017050.

West, P., & MADISON, W. (2005). Conference. *San Jose, CA.*

Xiao, F., Amirkhanian, A. N., & Amirkhanian, S. N. (2010). Influence of carbon nanoparticles on the rheological characteristics of short-term aged asphalt binders. *Journal of Materials in Civil Engineering, 23*(4), 423-431.

Xiao, F., Amirkhanian, S., & Juang, C. H. (2007). Rutting resistance of rubberized asphalt concrete pavements containing reclaimed asphalt pavement mixtures. *Journal of Materials in Civil Engineering, 19*(6), 475-483.

Xiao, F., Putman, B. J., & Amirkhanian, S. N. (2011). Viscosity prediction of CRM binders using artificial neural network approach. *International Journal of Pavement Engineering, 12*(5), 485-495.

Xu, T., & Huang, X. (2012). Investigation into causes of in-place rutting in asphalt pavement. *Construction and Building Materials, 28*(1), 525-530.

Yang, J., & Tighe, S. (2013). A review of advances of nanotechnology in asphalt mixtures.*Procedia-Social and Behavioral Sciences, 96*, 1269-1276.

Yildirim, Y. (2007). Polymer modified asphalt binders. *Construction and Building Materials, 21*(1), 66-72.

Yilmaz, M., Kok, B. V., Sengoz, B., Sengur, A., & Avci, E. (2011). Investigation of complex modulus of base and EVA modified bitumen with Adaptive-Network- Based Fuzzy Inference System. *Expert Systems with Applications, 38*(1), 969-974.

You, Z., Mills-Beale, J., Foley, J. M., Roy, S., Odegard, G. M., Dai, Q., & Goh, S. W. (2011). Nanoclay-modified asphalt materials: Preparation and characterization. *Construction and Building Materials, 25*(2), 1072-1078.

Yusoff, N. I. M., Breem, A. A. S., Alattug, H. N., Hamim, A., & Ahmad, J. (2014). The effects of moisture susceptibility and ageing conditions on nano-silica/polymer-modified asphalt mixtures. *Construction and Building Materials, 72*, 139-147.

Zhu, J., Birgisson, B., & Kringos, N. (2014). Polymer modification of bitumen: Advances and challenges. *European Polymer Journal, 54*, 18-38.

Ziari, H., Amini, A., Goli, A., & Mirzaeiyan, D. (2018). Predicting rutting performance of carbon nano tube (CNT) asphalt binders using regression models and neural networks. *Construction and Building Materials, 160*, 415-426.

APPENDICES

Appendix 1
The Data Used in The Modeling

Penetration	Softening point	Binder Type	Temperature in C	frequency in Hz	Strain in pa	|G*| in Pa	δ in
82	46	BASE ASPHLAT	46	0.159	1.2		
82	46	BASE ASPHLAT	46	0.2	1.2		
82	46	BASE ASPHLAT	46	0.5	1.2		
82	46	BASE ASPHLAT	46	1.592	1.2		
82	46	BASE ASPHLAT	46	2	1.2		
82	46	BASE ASPHLAT	46	3	1.2		
82	46	BASE ASPHLAT	46	5	1.2		
82	46	BASE ASPHLAT	46	10	1.2		
82	46	BASE ASPHLAT	46	15.92	1.2		
82	46	BASE ASPHLAT	52	0.159	1.2		
82	46	BASE ASPHLAT	52	0.2	1.2		
82	46	BASE ASPHLAT	52	0.5	1.2		
82	46	BASE ASPHLAT	52	1.592	1.2		

82	46	BASE ASPHLA T	52	2	1.2		
82	46	BASE ASPHLA T	52	3	1.2		
82	46	BASE ASPHLA T	52	5	1.2		
82	46	BASE ASPHLA T	52	10	1.2		
82	46	BASE ASPHLA T	52	15.92	1.2		
82	46	BASE ASPHLA T	58	0.159	1.2		
82	46	BASE ASPHLA T	58	0.2	1.2		
82	46	BASE ASPHLA T	58	0.5	1.2		
82	46	BASE ASPHLA T	58	1.592	1.2		
82	46	BASE ASPHLA T	58	2	1.2		
82	46	BASE ASPHLA T	58	3	1.2		
82	46	BASE ASPHLA T	58	5	1.2		
82	46	BASE ASPHLA T	58	10	1.2		
82	46	BASE ASPHLA T	58	15.92	1.2		
82	46	BASE ASPHLA T	64	0.159	1.2		

82	46	BASE ASPHLA T	64	0.2	1.2		
82	46	BASE ASPHLA T	64	0.5	1.2		
82	46	BASE ASPHLA T	64	1.592	1.2		
82	46	BASE ASPHLA T	64	2	1.2		
82	46	BASE ASPHLA T	64	3	1.2		
82	46	BASE ASPHLA T	64	5	1.2		
82	46	BASE ASPHLA T	64	10	1.2		
82	46	BASE ASPHLA T	64	15.92	1.2		
82	46	BASE ASPHLA T	70	0.159	1.2		
82	46	BASE ASPHLA T	70	0.2	1.2		
82	46	BASE ASPHLA T	70	0.5	1.2		
82	46	BASE ASPHLA T	70	1.592	1.2		
82	46	BASE ASPHLA T	70	2	1.2		
82	46	BASE ASPHLA T	70	3	1.2		
82	46	BASE ASPHLA T	70	5	1.2		

82	46	BASE ASPHLA T	70	10	1.2		
82	46	BASE ASPHLA T	70	15.92	1.2		
82	46	BASE ASPHLA T	76	0.159	1.2		
82	46	BASE ASPHLA T	76	0.2	1.2		
82	46	BASE ASPHLA T	76	0.5	1.2		
82	46	BASE ASPHLA T	76	1.592	1.2		
82	46	BASE ASPHLA T	76	2	1.2		
82	46	BASE ASPHLA T	76	3	1.2		
82	46	BASE ASPHLA T	76	5	1.2		
82	46	BASE ASPHLA T	76	10	1.2		
82	46	BASE ASPHLA T	76	15.92	1.2		
82	46	BASE ASPHLA T	82	0.159	1.2		
82	46	BASE ASPHLA T	82	0.2	1.2		
82	46	BASE ASPHLA T	82	0.5	1.2		
82	46	BASE ASPHLA T	82	1.592	1.2		

82	46	BASE ASPHLAT	82	2	1.2		
82	46	BASE ASPHLAT	82	3	1.2		
82	46	BASE ASPHLAT	82	5	1.2		
82	46	BASE ASPHLAT	82	10	1.2		
82	46	BASE ASPHLAT	82	15.92	1.2		
74	50	5% ASA	46	0.159	1.2		
74	50	5% ASA	46	0.2	1.2		
74	50	5% ASA	46	0.5	1.2		
74	50	5% ASA	46	1.592	1.2		
74	50	5% ASA	46	2	1.2		
74	50	5% ASA	46	3	1.2		
74	50	5% ASA	46	5	1.2		
74	50	5% ASA	46	10	1.2		
74	50	5% ASA	46	15.92	1.2		
74	50	5% ASA	52	0.159	1.2		
74	50	5% ASA	52	0.2	1.2		
74	50	5% ASA	52	0.5	1.2		
74	50	5% ASA	52	1.592	1.2		
74	50	5% ASA	52	2	1.2		
74	50	5% ASA	52	3	1.2		
74	50	5% ASA	52	5	1.2		
74	50	5% ASA	52	10	1.2		
74	50	5% ASA	52	15.92	1.2		
74	50	5% ASA	58	0.159	1.2		
74	50	5% ASA	58	0.2	1.2		
74	50	5% ASA	58	0.5	1.2		
74	50	5% ASA	58	1.592	1.2		
74	50	5% ASA	58	2	1.2		
74	50	5% ASA	58	3	1.2		
74	50	5% ASA	58	5	1.2		
74	50	5% ASA	58	10	1.2		
74	50	5% ASA	58	15.92	1.2		
74	50	5% ASA	64	0.159	1.2		

74	50	5% ASA	64	0.2	1.2		
74	50	5% ASA	64	0.5	1.2		
74	50	5% ASA	64	1.592	1.2		
74	50	5% ASA	64	2	1.2		
74	50	5% ASA	64	3	1.2		
74	50	5% ASA	64	5	1.2		
74	50	5% ASA	64	10	1.2		
74	50	5% ASA	64	15.92	1.2		
74	50	5% ASA	70	0.159	1.2		
74	50	5% ASA	70	0.2	1.2		
74	50	5% ASA	70	0.5	1.2		
74	50	5% ASA	70	1.592	1.2		
74	50	5% ASA	70	2	1.2		
74	50	5% ASA	70	3	1.2		
74	50	5% ASA	70	5	1.2		
74	50	5% ASA	70	10	1.2		
74	50	5% ASA	70	15.92	1.2		
74	50	5% ASA	76	0.159	1.2		
74	50	5% ASA	76	0.2	1.2		
74	50	5% ASA	76	0.5	1.2		
74	50	5% ASA	76	1.592	1.2		
74	50	5% ASA	76	2	1.2		
74	50	5% ASA	76	3	1.2		
74	50	5% ASA	76	5	1.2		
74	50	5% ASA	76	10	1.2		
74	50	5% ASA	76	15.92	1.2		
74	50	5% ASA	82	0.159	1.2		
74	50	5% ASA	82	0.2	1.2		
74	50	5% ASA	82	0.5	1.2		
74	50	5% ASA	82	1.592	1.2		
74	50	5% ASA	82	2	1.2		
74	50	5% ASA	82	3	1.2		
74	50	5% ASA	82	5	1.2		
74	50	5% ASA	82	10	1.2		
74	50	5% ASA	82	15.92	1.2		
66.4	56	3% ASA-COPPER	46	0.1592	1.2		
66.4	56	3% ASA-COPPER	46	0.2	1.2		
66.4	56	3% ASA-COPPER	46	0.5	1.2		

66.4	56	3% ASA-COPPER	46	1.592	1.2		
66.4	56	3% ASA-COPPER	46	2	1.2		
66.4	56	3% ASA-COPPER	46	3	1.2		
66.4	56	3% ASA-COPPER	46	5	1.2		
66.4	56	3% ASA-COPPER	46	10	1.2		
66.4	56	3% ASA-COPPER	46	15.92	1.2		
66.4	56	3% ASA-COPPER	52	0.1592	1.2		
66.4	56	3% ASA-COPPER	52	0.2	1.2		
66.4	56	3% ASA-COPPER	52	0.5	1.2		
66.4	56	3% ASA-COPPER	52	1.592	1.2		
66.4	56	3% ASA-COPPER	52	2	1.2		
66.4	56	3% ASA-COPPER	52	3	1.2		
66.4	56	3% ASA-COPPER	52	5	1.2		
66.4	56	3% ASA-COPPER	52	10	1.2		
66.4	56	3% ASA-COPPER	52	15.92	1.2		
66.4	56	3% ASA-COPPER	58	0.1592	1.2		
66.4	56	3% ASA-COPPER	58	0.2	1.2		
66.4	56	3% ASA-COPPER	58	0.5	1.2		
66.4	56	3% ASA-COPPER	58	1.592	1.2		
66.4	56	3% ASA-COPPER	58	2	1.2		
66.4	56	3% ASA-COPPER	58	3	1.2		
66.4	56	3% ASA-COPPER	58	5	1.2		
66.4	56	3% ASA-COPPER	58	10	1.2		

66.4	56	3% ASA-COPPER	58	15.92	1.2		
66.4	56	3% ASA-COPPER	64	0.1592	1.2		
66.4	56	3% ASA-COPPER	64	0.2	1.2		
66.4	56	3% ASA-COPPER	64	0.5	1.2		
66.4	56	3% ASA-COPPER	64	1.592	1.2		
66.4	56	3% ASA-COPPER	64	2	1.2		
66.4	56	3% ASA-COPPER	64	3	1.2		
66.4	56	3% ASA-COPPER	64	5	1.2		
66.4	56	3% ASA-COPPER	64	10	1.2		
66.4	56	3% ASA-COPPER	64	15.92	1.2		
66.4	56	3% ASA-COPPER	70	0.1592	1.2		
66.4	56	3% ASA-COPPER	70	0.2	1.2		
66.4	56	3% ASA-COPPER	70	0.5	1.2		
66.4	56	3% ASA-COPPER	70	1.592	1.2		
66.4	56	3% ASA-COPPER	70	2	1.2		
66.4	56	3% ASA-COPPER	70	3	1.2		
66.4	56	3% ASA-COPPER	70	5	1.2		
66.4	56	3% ASA-COPPER	70	10	1.2		
66.4	56	3% ASA-COPPER	70	15.92	1.2		
66.4	56	3% ASA-COPPER	76	0.1592	1.2		
66.4	56	3% ASA-COPPER	76	0.2	1.2		
66.4	56	3% ASA-COPPER	76	0.5	1.2		
66.4	56	3% ASA-COPPER	76	1.592	1.2		

66.4	56	3% ASA-COPPER	76	2	1.2		
66.4	56	3% ASA-COPPER	76	3	1.2		
66.4	56	3% ASA-COPPER	76	5	1.2		
66.4	56	3% ASA-COPPER	76	10	1.2		
66.4	56	3% ASA-COPPER	76	15.92	1.2		
66.4	56	3% ASA-COPPER	82	0.1592	1.2		
66.4	56	3% ASA-COPPER	82	0.2	1.2		
66.4	56	3% ASA-COPPER	82	0.5	1.2		
66.4	56	3% ASA-COPPER	82	1.592	1.2		
66.4	56	3% ASA-COPPER	82	2	1.2		
66.4	56	3% ASA-COPPER	82	3	1.2		
66.4	56	3% ASA-COPPER	82	5	1.2		
66.4	56	3% ASA-COPPER	82	10	1.2		
66.4	56	3% ASA-COPPER	82	15.92	1.2		
75.3	55	3% ASA-KAL	46	0.159	1.2		
75.3	55	3% ASA-KAL	46	0.2	1.2		
75.3	55	3% ASA-KAL	46	0.5	1.2		
75.3	55	3% ASA-KAL	46	1.592	1.2		
75.3	55	3% ASA-KAL	46	2	1.2		
75.3	55	3% ASA-KAL	46	3	1.2		
75.3	55	3% ASA-KAL	46	5	1.2		
75.3	55	3% ASA-KAL	46	10	1.2		
75.3	55	3% ASA-KAL	46	15.92	1.2		

75.3	55	3% ASA-KAL	52	0.159	1.2		
75.3	55	3% ASA-KAL	52	0.2	1.2		
75.3	55	3% ASA-KAL	52	0.5	1.2		
75.3	55	3% ASA-KAL	52	1.592	1.2		
75.3	55	3% ASA-KAL	52	2	1.2		
75.3	55	3% ASA-KAL	52	3	1.2		
75.3	55	3% ASA-KAL	52	5	1.2		
75.3	55	3% ASA-KAL	52	10	1.2		
75.3	55	3% ASA-KAL	52	15.92	1.2		
75.3	55	3% ASA-KAL	58	0.159	1.2		
75.3	55	3% ASA-KAL	58	0.2	1.2		
75.3	55	3% ASA-KAL	58	0.5	1.2		
75.3	55	3% ASA-KAL	58	1.592	1.2		
75.3	55	3% ASA-KAL	58	2	1.2		
75.3	55	3% ASA-KAL	58	3	1.2		
75.3	55	3% ASA-KAL	58	5	1.2		
75.3	55	3% ASA-KAL	58	10	1.2		
75.3	55	3% ASA-KAL	58	15.92	1.2		
75.3	55	3% ASA-KAL	64	0.159	1.2		
75.3	55	3% ASA-KAL	64	0.2	1.2		
75.3	55	3% ASA-KAL	64	0.5	1.2		
75.3	55	3% ASA-KAL	64	1.592	1.2		
75.3	55	3% ASA-KAL	64	2	1.2		

75.3	55	3% ASA-KAL	64	3	1.2		
75.3	55	3% ASA-KAL	64	5	1.2		
75.3	55	3% ASA-KAL	64	10	1.2		
75.3	55	3% ASA-KAL	64	15.92	1.2		
75.3	55	3% ASA-KAL	70	0.159	1.2		
75.3	55	3% ASA-KAL	70	0.2	1.2		
75.3	55	3% ASA-KAL	70	0.5	1.2		
75.3	55	3% ASA-KAL	70	1.592	1.2		
75.3	55	3% ASA-KAL	70	2	1.2		
75.3	55	3% ASA-KAL	70	3	1.2		
75.3	55	3% ASA-KAL	70	5	1.2		
75.3	55	3% ASA-KAL	70	10	1.2		
75.3	55	3% ASA-KAL	70	15.92	1.2		
75.3	55	3% ASA-KAL	76	0.159	1.2		
75.3	55	3% ASA-KAL	76	0.2	1.2		
75.3	55	3% ASA-KAL	76	0.5	1.2		
75.3	55	3% ASA-KAL	76	1.592	1.2		
75.3	55	3% ASA-KAL	76	2	1.2		
75.3	55	3% ASA-KAL	76	3	1.2		
75.3	55	3% ASA-KAL	76	5	1.2		
75.3	55	3% ASA-KAL	76	10	1.2		
75.3	55	3% ASA-KAL	76	15.92	1.2		
75.3	55	3% ASA-KAL	82	0.159	1.2		

75.3	55	3% ASA-KAL	82	0.2	1.2		
75.3	55	3% ASA-KAL	82	0.5	1.2		
75.3	55	3% ASA-KAL	82	1.592	1.2		
75.3	55	3% ASA-KAL	82	2	1.2		
75.3	55	3% ASA-KAL	82	3	1.2		
75.3	55	3% ASA-KAL	82	5	1.2		
75.3	55	3% ASA-KAL	82	10	1.2		
75.3	55	3% ASA-KAL	82	15.92	1.2		
75.3	55	3% ASA-KAL	82	15.92	1.2		
69.1	55	5% ASA-COPPER	46	0.159	1.2		
69.1	55	5% ASA-COPPER	46	0.2	1.2		
69.1	55	5% ASA-COPPER	46	0.5	1.2		
69.1	55	5% ASA-COPPER	46	1.592	1.2		
69.1	55	5% ASA-COPPER	46	2	1.2		
69.1	55	5% ASA-COPPER	46	3	1.2		
69.1	55	5% ASA-COPPER	46	5	1.2		
69.1	55	5% ASA-COPPER	46	10	1.2		
69.1	55	5% ASA-COPPER	46	15.92	1.2		
69.1	55	5% ASA-COPPER	52	0.159	1.2		
69.1	55	5% ASA-COPPER	52	0.2	1.2		
69.1	55	5% ASA-COPPER	52	0.5	1.2		
69.1	55	5% ASA-COPPER	52	1.592	1.2		
69.1	55	5% ASA-COPPER	52	2	1.2		

69.1	55	5% ASA-COPPER	52	3	1.2		
69.1	55	5% ASA-COPPER	52	5	1.2		
69.1	55	5% ASA-COPPER	52	10	1.2		
69.1	55	5% ASA-COPPER	52	15.92	1.2		
69.1	55	5% ASA-COPPER	58	0.159	1.2		
69.1	55	5% ASA-COPPER	58	0.2	1.2		
69.1	55	5% ASA-COPPER	58	0.5	1.2		
69.1	55	5% ASA-COPPER	58	1.592	1.2		
69.1	55	5% ASA-COPPER	58	2	1.2		
69.1	55	5% ASA-COPPER	58	3	1.2		
69.1	55	5% ASA-COPPER	58	5	1.2		
69.1	55	5% ASA-COPPER	58	10	1.2		
69.1	55	5% ASA-COPPER	58	15.92	1.2		
69.1	55	5% ASA-COPPER	64	0.159	1.2		
69.1	55	5% ASA-COPPER	64	0.2	1.2		
69.1	55	5% ASA-COPPER	64	0.5	1.2		
69.1	55	5% ASA-COPPER	64	1.592	1.2		
69.1	55	5% ASA-COPPER	64	2	1.2		
69.1	55	5% ASA-COPPER	64	3	1.2		
69.1	55	5% ASA-COPPER	64	5	1.2		
69.1	55	5% ASA-COPPER	64	10	1.2		
69.1	55	5% ASA-COPPER	64	15.92	1.2		
69.1	55	5% ASA-COPPER	70	0.159	1.2		

69.1	55	5% ASA-COPPER	70	0.2	1.2		
69.1	55	5% ASA-COPPER	70	0.5	1.2		
69.1	55	5% ASA-COPPER	70	1.592	1.2		
69.1	55	5% ASA-COPPER	70	2	1.2		
69.1	55	5% ASA-COPPER	70	3	1.2		
69.1	55	5% ASA-COPPER	70	5	1.2		
69.1	55	5% ASA-COPPER	70	10	1.2		
69.1	55	5% ASA-COPPER	70	15.92	1.2		
69.1	55	5% ASA-COPPER	76	0.159	1.2		
69.1	55	5% ASA-COPPER	76	0.2	1.2		
69.1	55	5% ASA-COPPER	76	0.5	1.2		
69.1	55	5% ASA-COPPER	76	1.592	1.2		
69.1	55	5% ASA-COPPER	76	2	1.2		
69.1	55	5% ASA-COPPER	76	3	1.2		
69.1	55	5% ASA-COPPER	76	5	1.2		
69.1	55	5% ASA-COPPER	76	10	1.2		
69.1	55	5% ASA-COPPER	76	15.92	1.2		
69.1	55	5% ASA-COPPER	82	0.159	1.2		
69.1	55	5% ASA-COPPER	82	0.2	1.2		
69.1	55	5% ASA-COPPER	82	0.5	1.2		
69.1	55	5% ASA-COPPER	82	1.592	1.2		
69.1	55	5% ASA-COPPER	82	2	1.2		
69.1	55	5% ASA-COPPER	82	3	1.2		

69.1	55	5% ASA-COPPER	82	5	1.2		
69.1	55	5% ASA-COPPER	82	10	1.2		
69.1	55	5% ASA-COPPER	82	15.92	1.2		
76.9	53	5% ASA-KAL	46	0.159	1.2		
76.9	53	5% ASA-KAL	46	0.2	1.2		
76.9	53	5% ASA-KAL	46	0.5	1.2		
76.9	53	5% ASA-KAL	46	1.592	1.2		
76.9	53	5% ASA-KAL	46	2	1.2		
76.9	53	5% ASA-KAL	46	3	1.2		
76.9	53	5% ASA-KAL	46	5	1.2		
76.9	53	5% ASA-KAL	46	10	1.2		
76.9	53	5% ASA-KAL	46	15.92	1.2		
76.9	53	5% ASA-KAL	52	0.159	1.2		
76.9	53	5% ASA-KAL	52	0.2	1.2		
76.9	53	5% ASA-KAL	52	0.5	1.2		
76.9	53	5% ASA-KAL	52	1.592	1.2		
76.9	53	5% ASA-KAL	52	2	1.2		
76.9	53	5% ASA-KAL	52	3	1.2		
76.9	53	5% ASA-KAL	52	5	1.2		
76.9	53	5% ASA-KAL	52	10	1.2		
76.9	53	5% ASA-KAL	52	15.92	1.2		
76.9	53	5% ASA-KAL	58	0.159	1.2		
76.9	53	5% ASA-KAL	58	0.2	1.2		

76.9	53	5% ASA-KAL	58	0.5	1.2		
76.9	53	5% ASA-KAL	58	1.592	1.2		
76.9	53	5% ASA-KAL	58	2	1.2		
76.9	53	5% ASA-KAL	58	3	1.2		
76.9	53	5% ASA-KAL	58	5	1.2		
76.9	53	5% ASA-KAL	58	10	1.2		
76.9	53	5% ASA-KAL	58	15.92	1.2		
76.9	53	5% ASA-KAL	64	0.159	1.2		
76.9	53	5% ASA-KAL	64	0.2	1.2		
76.9	53	5% ASA-KAL	64	0.5	1.2		
76.9	53	5% ASA-KAL	64	1.592	1.2		
76.9	53	5% ASA-KAL	64	2	1.2		
76.9	53	5% ASA-KAL	64	3	1.2		
76.9	53	5% ASA-KAL	64	5	1.2		
76.9	53	5% ASA-KAL	64	10	1.2		
76.9	53	5% ASA-KAL	64	15.92	1.2		
76.9	53	5% ASA-KAL	70	0.159	1.2		
76.9	53	5% ASA-KAL	70	0.2	1.2		
76.9	53	5% ASA-KAL	70	0.5	1.2		
76.9	53	5% ASA-KAL	70	1.592	1.2		
76.9	53	5% ASA-KAL	70	2	1.2		
76.9	53	5% ASA-KAL	70	3	1.2		
76.9	53	5% ASA-KAL	70	5	1.2		

76.9	53	5% ASA-KAL	70	10	1.2		
76.9	53	5% ASA-KAL	70	15.92	1.2		
76.9	53	5% ASA-KAL	76	0.159	1.2		
76.9	53	5% ASA-KAL	76	0.2	1.2		
76.9	53	5% ASA-KAL	76	0.5	1.2		
76.9	53	5% ASA-KAL	76	1.592	1.2		
76.9	53	5% ASA-KAL	76	2	1.2		
76.9	53	5% ASA-KAL	76	3	1.2		
76.9	53	5% ASA-KAL	76	5	1.2		
76.9	53	5% ASA-KAL	76	10	1.2		
76.9	53	5% ASA-KAL	76	15.92	1.2		
76.9	53	5% ASA-KAL	82	0.159	1.2		
76.9	53	5% ASA-KAL	82	0.2	1.2		
76.9	53	5% ASA-KAL	82	0.5	1.2		
76.9	53	5% ASA-KAL	82	1.592	1.2		
76.9	53	5% ASA-KAL	82	2	1.2		
76.9	53	5% ASA-KAL	82	3	1.2		
76.9	53	5% ASA-KAL	82	5	1.2		
76.9	53	5% ASA-KAL	82	10	1.2		
76.9	53	5% ASA-KAL	82	15.92	1.2		
76.9	53	5% ASA-KAL	82	10	1.2		
76.9	53	5% ASA-KAL	82	15.92	1.2		

Appendix 2
Ethical Approval Latter

NEAR EAST UNIVERSITY YAKIN DOĞU ÜNİVERSİTESİ

REF:5/8/2020

ETHICS APPROVAL LETTER

TO GRADUATE SCHOOL OF APPLİED SCİENCES

REFERENCE: MSC. GAZI F. G. TALLAWI

I would like to inform you that the above candidate is one of our postgraduate students in Civil Engineering department he is taking thesis under my supervision and the thesis entailed: ***Modeling Of Different Nano-Composite Modified Bitumen Using Computational Intelligence-An Ensemble Learning Approach***. The data used in his study was our own data obtinated from experimental work conducted by me in Malaysia.

Please do not hesitate to contact me if you have any further queries or questions.

Thank you very much indeed.

Best Regards,

Dr. Shaban Isamel Albrka
Civil Engineering Department,
Faculty of Civil and Environmental Engineering,
Near East Boulevard, ZIP: 99138
Nicosia / TRNC, North Cyprus,
Mersin 10 – Turkey.
Email: shabanismeal.albrka@neu.edu.tr

Appendix 3
Similarity Report

Assignments | Students | Grade Book | Libraries | Calendar | Discussion | Preferences

NOW VIEWING: HOME > MY PAPERS > PAPER

About this page

This is your assignment inbox. To view a paper, select the paper's title. To view a Similarity Report, select the paper's Similarity Report icon in the similarity column. A ghosted icon indicates that the Similarity Report has not yet been generated.

paper

INBOX | NOW VIEWING: NEW PAPERS ▾

Submit File

Online Grading Report | Edit assignment settings | Email non-submitters

AUTHOR	TITLE	SIMILARITY	GRADE	RESPONSE	FILE	PAPER ID	DATE
Gazi Tallawi	Abstract	0%	--	--		1360395628	21-Jul-2020
Gazi Tallawi	ch4	0%	--	--		1360395204	21-Jul-2020
Gazi Tallawi	CH5	0%	--	--		1360395371	21-Jul-2020
Gazi Tallawi	CH1	11%	--	--		1359971000	20-Jul-2020
Gazi Tallawi	CH2	13%	--	--		1359971266	20-Jul-2020
Gazi Tallawi	CH3	13%	--	--		1359971497	20-Jul-2020
Gazi Tallawi	Thesis	15%	--	--		1360732752	22-Jul-2020

Dr. Shaban Ismael Albrka
22/07/2020